

## DYNAMICS AND NONCLASSICAL PHOTON STATISTICS IN THE INTERACTION OF TWO-LEVEL SPIN SYSTEMS WITH A TWO-MODE CAVITY FIELD. A GENERALIZED JAYNES-CUMMINGS MODEL

HORACIO GRINBERG\*

*Departamento de Física, Facultad de Ciencias Exactas y Naturales,  
Universidad de Buenos Aires, Pabellón 1, Ciudad Universitaria,  
(1428) Buenos Aires, Argentina<sup>†</sup>  
grinberg@df.uba.ar*

Received 7 January 2007

The interaction of a two-level  $XY$   $n$ -spin system with a two-mode cavity field is investigated through a generalized Jaynes-Cummings model in the rotating wave approximation. The spontaneous decay of a spin level was treated by considering the interaction of the two-level spin system with the modes of the universe in the vacuum state. The different cases of interest, characterized in terms of a detuning parameter for each mode, which emerge from the nonvanishing of certain commutation relations between interaction picture Hamiltonians associated with each mode, were analytically implemented and numerically discussed for various values of the initial mean photon number and spin-photon coupling constants. Photon distribution, time evolution of the spin population inversion, as well as the statistical properties of the field leading to the possible production of nonclassical states, such as antibunched light and violations of the Cauchy-Schwartz inequality are examined for an excited initial state. It was assumed that the two modes are initially in coherent states and have the same photon distribution. The case of zero detuning of both modes was treated in terms of a linearization of the expansion of the time evolution operator, while in other three cases, the computations were conducted via second- and third-order Dyson perturbation expansion of the time evolution operator matrix elements for the excited and ground states respectively.

*Keywords:* Spin models; two-level systems; two-mode interaction; quantum optics; nonclassical effects; field statistics.

PACS numbers: 03.65.Ca, 42.50.-p, 42.50.Ar, 42.50.Pq, 42.50.Dv

### 1. Introduction

A two-level system interacting with a radiation field provides a centrally important simplified quantum model for the interaction of radiation and matter.<sup>1,2</sup> In

\*Member of the Consejo Nacional de Investigaciones Científicas y Técnicas (CONICET), República Argentina.

<sup>†</sup>Permanent address.

particular, the Jaynes-Cummings model<sup>3</sup> (JCM) of a two-level atom interacting with a quantized single-mode electromagnetic field<sup>4</sup> is at the core of many problems in quantum optics, NMR, and quantum electronics. The importance of this model lies in that it is perhaps the simplest solvable model that describes the essential physics of radiation-matter interaction. Earlier studies of this model by Eberly *et al.*,<sup>5-7</sup> Stenholm<sup>8</sup> and Gou<sup>9</sup> involving an electromagnetic field initially in a coherent state have revealed the periodic collapse and revival of Rabi oscillations, which are clearly a manifestation of the role of quantum mechanics in the coherence and fluctuation properties of radiation-matter systems. An exactly solvable model of atom-phonon coupling showing periodic decay and revival has been reported by Buck and Sukumar,<sup>10</sup> and the relations between photon statistical characteristics and atomic level populations were examined rigorously in a two-mode model by Bogolubov *et al.*<sup>11</sup> More generally, the phenomenon of collapses and revivals of Rabi oscillations was studied for a two-level atom undergoing either one- or two-photon transitions in a two-mode squeezed state field.<sup>12-14</sup> Recent technological advances in quantum optics such as the development of experiments in high-Q superconductivity cavities<sup>15,16</sup> has demonstrated the existence of these interesting nonclassical properties and stimulated the interest of studying the JCM and its various generalizations in greater detail. This model is not only physically realistic, but mathematically tractable, in the so-called rotating-wave approximation, widely used in the quantum optics master equation<sup>17</sup> and validated for all cases of practical interest many decades ago.<sup>18</sup> It is recognized as one of the exactly solvable, fully quantum mechanical models describing the interaction of matter with an electromagnetic field<sup>19</sup> and with quantized fields in a leaky cavity.<sup>20</sup> Not only does the JCM provide a fundamental description of a two-level system in a quantized field, it is also an important tool for controlling quantum states.<sup>21</sup> The cavity field can be regarded as a quantum probe of the dressed states defined by the classical laser field.

Many interesting effects associated with similar systems of fields and two-level models have been predicted and observed in the past, for example, two-photon gain,<sup>22,23</sup> cavity perturbed resonance fluorescence spectra,<sup>24</sup> atomic squeezing in the cavity,<sup>25</sup> and very large decoherence time related to some ramifications of the quantum Hall effect.<sup>26</sup> The effects emerging from these events are particularly relevant because of their potential applications in quantum computation with solid-state quantum bits processing,<sup>27</sup> semiconductor and quantum information devices<sup>28-30</sup> as well as in realizations of optical communication,<sup>31</sup> laser cooling of atoms,<sup>32</sup> etc. More recently, the dynamics of a two-level system by laser pulses has been investigated.<sup>33</sup>

Over the past decade, there has been much interest in the quantum dynamics of two-level systems with two modes of a quantized cavity field.<sup>34,35</sup> An example of such a system is the generalized JCM, in which the atomic transitions are mediated by nondegenerate two-photon absorption or emission.<sup>9</sup> However, for certain variants

of the Jaynes-Cummings non-phenomenological Hamiltonians, incorporation of two laser fields with different amplitudes and frequencies in the quantum regime resists an exact analytical solution, even in the case of exact simultaneous resonance of the two-level system with both modes of the cavity field.

Although there has been a lot of previous work dealing with both the response of two-level atoms to dual frequency semiclassical excitation in the steady-state regime<sup>36,37</sup> and with the transient regime with a quantum probe field,<sup>9,14,20,34,35,38,39</sup> a systematic analysis concerning the degenerate and nondegenerate two-mode nonclassical states associated with the resonant and off-resonant states of the cavity field with the spin system is not completely documented so far, and this motivates us to introduce in this paper a generalized JCM in which the transitions are mediated by two modes of photons in resonant and off-resonant states. This paper extends earlier studies of the transient dynamics of a two-level  $n$ -spin model interacting with a single mode quantized cavity field.<sup>40-42</sup> Here, the quantum dynamics of this system interacting with correlated two-mode field states is investigated through a generalized JCM, in which the spin cyclic system is that described in the classical paper by Lieb, Schultz, and Mattis (LSM).<sup>43</sup> In a recent paper, some preliminary results were reported in off-resonant states of the two-mode cavity field with this spin system.<sup>44</sup> In the present work, the interaction of this spin model with a two-mode cavity field in the quantum regime is investigated in the rotating wave approximation through a *linearization* of the expansion of the time evolution operator in the case of exact simultaneous resonance of both modes of the cavity field with the spin transition frequency. In off-resonant states, on the other hand, the interaction picture non-phenomenological Hamiltonian of the model becomes time-dependent. Moreover, since in this case the set of interaction picture Hamiltonians  $\mathcal{V}(t_1), \mathcal{V}(t_2), \dots$ , taken at different times  $t_1, t_2, \dots$  fail to commute, Dyson perturbation expansion of the time evolution operator matrix elements truncated to a finite order has to be used in these cases. The system dynamics will be developed through the probability amplitudes and the density operator formalism, assuming that the field modes are initially in coherent states and the spin system is in the excited state with the initial coherent state of the field given by Poisson and Gaussian distributions. Analytical expressions of the probability amplitudes are given for both resonant and off-resonant states involving degenerate and nondegenerate modes of the cavity field. These are discussed in terms of a detuning parameter for each mode. The detunings between the cavity mode and the spin transition can have an important influence on the nonclassical effects, as recently reported in the case of a two-level atom coupled to a single mode of cavity fields.<sup>45</sup> The main advantage of the present model is that one can use one mode to modulate or control the output of the other mode. Thus, the collapse and revivals of the population inversion can be controlled by the detunings between the cavity mode and the spin transition. Another important aspect of the present model is the possibility of exploring the temperature dependence on the detuning parameters through the explicit incorporation of a thermal photon state for each mode.<sup>40-42</sup>

The superposition states from several two-mode coherent states were reported, and it was shown that under certain conditions, the superposition states may exhibit nonclassical effects, such as photon antibunching, sub-Poissonian photon statistics, squeezing, and violation of the Cauchy-Schwartz inequality.<sup>35,46–48</sup> Thus, the main focus of attention in this paper is not only on the the photon distribution and population dynamics (actually the spin inversion), but some aspects of the dynamics of the field statistics exhibiting nonclassical properties, such as the possible production of antibunched states and violations of the Cauchy-Schwartz inequality, will also be investigated in some detail. Although the general formalism involving the possibility of squeezing coherent states will be discussed in a forthcoming paper, one calculation with a photon distribution function for an ideal squeezed state describing the initial coherent state is performed, which indeed clearly shows the violation of the Cauchy-Schwartz inequality.

This paper is organized as follows. Section 2 briefly describes the cyclic spin system considered, based on the model investigated by LSM.<sup>43</sup> Complete analytical details on the thermally averaged procedure involving non-orthogonal Grassmann coherent states to generate a manifold of excited states, by allowing one to treat the model as a Jaynes-Cummings two-level system, and thus opening the possibility of exploring the dynamics in off-resonant states, are described in previous papers.<sup>40–42</sup> In Sec. 3, the interaction of this spin system with a quantized cavity field is analyzed in the interaction picture representation, which is a competent scenario to generate explicit expressions of dynamical properties. The interaction picture Hamiltonian of the model can be divided into two parts (one for each mode) and these two parts do not commute with each other. Moreover, since the sum of these operators taken at different times fail to commute, except in the (nontrivial) particular case of exact simultaneous resonance of both modes with the spin transition frequency, there are in all four cases of interest concerning the different relations between the detuning parameters. These four cases are given analytical expressions of the probability amplitudes through the density operator formalism. In Sec. 4, the photon distribution of the cavity field as well as the spin inversion dynamics of the model are discussed for both degenerate and nondegenerate modes of the cavity field in resonant and off-resonant states, and for different values of the mean number of photons. In particular, the spin inversion and the dynamics of the field statistics both play an important role in view of the possibility that nonclassical states might be generated by the interaction. Many of the existing theoretical studies on the JCM are restricted to the detailed discussion on single- and two-mode interaction in resonant states. In the present investigation, we shall study the influence of the detuning parameters on these nonclassical effects, such as the variance of the two-mode quadrature operator of the fields and of the Cauchy-Schwartz inequality. It is further shown that the number of configurations of a given multiplicity is perfectly consistent with the dimension of the trace of the unit operator in a basis of Grassmann generators.<sup>40,41</sup> This is an important issue because all the states derived from the totality of spin adapted configurations have to be included in the computation

of the spin transition frequency in off-resonant states of both modes. Finally, the temperature distribution in off-resonant states and in the isotropic limit of the spin system is briefly discussed in the limit of high and low temperatures. Section 5 concludes the paper with a brief summary and some discussion.

### 2. Cyclic XY Spin Model

In a previous paper,<sup>40,41</sup> the XY  $n$ -spin cyclic model, as described by LSM<sup>43</sup> via the Hamiltonian

$$\mathcal{H}_\gamma(n^\dagger, n) = \sum_k \Xi_k n_k^\dagger n_k - \frac{1}{2} \sum_k \Xi_k, \tag{1}$$

was investigated by means of a functional integral representation involving non-orthogonal Grassmann (anticommuting) coherent states integration variables.<sup>49,50</sup> In Eq. (1),  $n^\dagger, n$  are fermionic operators and the  $\Xi_k$  are the associated eigenvalues, given by<sup>43</sup>

$$\Xi_k^2 = 1 - (1 - \gamma^2) \sin^2 k, \tag{2}$$

where  $\gamma$  is a parameter characterizing the degree of anisotropy in the  $xy$ -plane and where

$$k = 2\pi p/n, \quad p = -1/2n \dots, 0, 1, \dots, 1/2n - 1. \tag{3}$$

Use of the completeness relation of the  $n$ -site Grassmann states, invoking antiperiodic boundary conditions, performing an analytic continuation to Euclidean times, and the subsequent substitution  $\Delta\tau/\hbar \rightarrow \beta$  ( $\equiv 1/K_B T$ ) in the functional integral, allowed the imaginary time partition function of this model to be obtained as a configuration expansion through the trace formula for fermions. In this scenario, the energy of the model emerges as<sup>40,41</sup>

$$\Xi(n; \beta; \gamma) = -1/2 \sum_k \Xi_k - \frac{\partial}{\partial \beta} \ln \left( 1 + \sum_{m=1}^n S(m) \right), \tag{4}$$

where the  $m$ th configuration in the expansion becomes

$$S(m) = \sum_{\alpha_1 > \alpha_2 > \dots > \alpha_m = 1} \prod_{j=1}^m \exp(-\beta \Xi_{\alpha_j}). \tag{5}$$

Discussion of the sign of  $\Xi_k$  in Eq. (2) as well as the possibility of the existence of null eigenvalues are discussed in Ref. 43. In this paper, only positive values of  $\Xi_k$  will be considered. As noted by LSM, this corresponds to a particle-hole picture for the  $n$ -particles, where the ground state has no elementary fermions and the elementary fermion excitations both above and below the Fermi surface have positive energies.

### 3. Interaction with a Quantized Cavity Field

In a previous paper,<sup>40,41</sup> it was shown that the two-level  $n$ -spin system is characterized by the ground state  $|0\rangle \equiv |a\rangle$  and a thermally averaged manifold of excited states  $|b\rangle$ . By using the completeness relation  $|a\rangle\langle a| + |b\rangle\langle b| \equiv \sigma_{aa} + \sigma_{bb} = 1$ , the Hamiltonian (1) can be written as

$$\mathcal{H}_\gamma(n^\dagger, n) = \hbar\omega_a \bigotimes_1^n |0\rangle\langle 0| + \hbar\omega_b \bigotimes_1^n |b\rangle\langle b|, \tag{6}$$

where  $\mathcal{H}_\gamma|a\rangle = \hbar\omega_a|a\rangle$  and  $\mathcal{H}_\gamma|b\rangle = \hbar\omega_b|b\rangle$ . The eigenvalues  $\omega_a$  and  $\omega_b$  represent the energies of the ground and excited states respectively, given by

$$\hbar\omega_a = \langle 0|\mathcal{H}_\gamma(n^\dagger, n)|0\rangle = -1/2 \sum_k \Xi_k, \tag{7}$$

and

$$\hbar\omega_b = \frac{\partial}{\partial\beta} \ln \left[ \text{Tr} \exp \left( -\beta \sum_k \Xi_k n^\dagger, n_k \right) \right]^{-1}. \tag{8}$$

With the help of the definition of  $\sigma_z$ , written here in terms of the diagonal projection operators  $\sigma_{aa}$  and  $\sigma_{bb}$  as

$$\sigma_z = \bigotimes (|b\rangle\langle b| - |a\rangle\langle a|), \tag{9}$$

Eq. (6) is transformed to

$$\mathcal{H}_\gamma(n^\dagger, n) = 1/2\hbar\omega\sigma_z + 1/2\hbar(\omega_a + \omega_b)I, \tag{10}$$

where  $I$  is the unit operator in the appropriate  $n$ -dimensional space and  $\omega = \omega_b - \omega_a$  is the spin transition frequency. Introducing the raising and lowering spin operators, given in terms of the spin transition operators  $\sigma_{ba}$  and  $\sigma_{ab}$ , we write these operators for  $n$  degrees of freedom as a direct product

$$\sigma_+ = \bigotimes_1^n \sigma_{ba} \equiv \bigotimes_1^n |b\rangle\langle 0|, \tag{11}$$

$$\sigma_- = \bigotimes_1^n \sigma_{ab} \equiv \bigotimes_1^n |0\rangle\langle b|, \tag{12}$$

satisfying the same commutation relations as the spin  $-1/2$  algebra of the Pauli matrices and therefore constitute a basis of the direct product of  $SU(2)$  algebra. Thus, the complete Hamiltonian of the spin system and the cavity field can be written as

$$\mathcal{H} = \hbar \sum_{j=1}^2 \nu_j (\langle m_j \rangle; \beta) a_j^\dagger a_j + \frac{1}{2} \hbar \omega \sigma_z + \hbar \sum_{j=1}^2 g_j (\sigma_+ + \sigma_-) (a_j + a_j^\dagger), \tag{13}$$

where  $g_j$  is the spin-field coupling constant for the mode  $j$ , the zero-point energy of the bosonic field was omitted and the constant term  $1/2(\omega_a + \omega_b)$  in Eq. (10) was

ignored.  $\sigma_{\pm}$ ,  $\sigma_z$  are the spin flip operators characterizing the effective two-level spin system with transition frequency  $\omega$  and  $a_j^\dagger$ ,  $a_j$  are bosonic creation and annihilation operators of cavity modes. It is assumed that the field is in a thermal photon state in which  $\nu_j(\langle m_j \rangle; \beta)$  is the photon frequency for the mode  $j$ , given in terms of the mean number of photons  $\langle m_j \rangle$  in the cavity field by

$$\nu_j(\langle m_j \rangle; \beta) = \frac{1}{\hbar\beta} \ln \left( \frac{1 + \langle m_j \rangle}{\langle m_j \rangle} \right). \tag{14}$$

Dropping the energy nonconserving terms  $a_j\sigma_-$  and  $a_j^\dagger\sigma_+$  in Eq. (13) corresponds to the rotating-wave approximation. It amounts to the neglect of a small shift in the resonance frequency, a shift that depends on the strength of the interaction with the radiation field.<sup>51</sup> It follows that the interaction of a two-mode quantized field of frequency  $\nu_j(\langle m_j \rangle; \beta)$  with a two-level spin system is described by the Hamiltonian

$$\mathcal{H} = \mathcal{H}_0 + \mathcal{H}_1, \tag{15}$$

where  $\mathcal{H}_0$  and  $\mathcal{H}_1$  can be expressed in terms of the direct product generators

$$\mathcal{H}_0 = \hbar \sum_{j=1}^2 \left( \nu_j(\langle m_j \rangle; \beta) a_j^\dagger a_j \otimes I \right) + I \otimes \mathcal{H}_\gamma(n^\dagger, n), \tag{16}$$

$$\mathcal{H}_1 = \hbar \sum_{j=1}^2 g_j \left[ \left( \sigma_+ \otimes I \right) \cdot \left( I \otimes a_j \right) + \left( a_j^\dagger \otimes I \right) \cdot \left( I \otimes \sigma_- \right) \right]. \tag{17}$$

It is convenient to work in the interaction picture. Introducing the unitary time-evolution operator for the unperturbed Hamiltonian

$$U_0(t) = \exp \left( -\frac{i}{\hbar} \mathcal{H}_0 t \right), \tag{18}$$

which merely contributes a phase factor in each spin subspace, the interaction picture Hamiltonian is given by

$$\mathcal{V}(t) = U_0^\dagger(t) \mathcal{H}_1 U_0(t). \tag{19}$$

Using the expansion

$$e^{\alpha A} B e^{-\alpha A} = B + \alpha [A, B] + \frac{\alpha^2}{2!} [A, [A, B]] + \dots, \tag{20}$$

and consequently noting that

$$e^{i\nu_j a_j^\dagger a_j t} a_j e^{-i\nu_j a_j^\dagger a_j t} = a_j e^{-i\nu_j t}, \tag{21}$$

$$e^{i\omega\sigma_z t/2} \sigma_+ e^{-i\omega\sigma_z t/2} = \sigma_+ e^{i\omega t}, \tag{22}$$

the interaction picture Hamiltonian can be written, invoking the rotating wave approximation and after standard manipulations, as

$$\mathcal{V}(t) \equiv \mathcal{V}_1(t) + \mathcal{V}_2(t) = \hbar \sum_{j=1}^2 g_j \left( \sigma_+ a_j e^{i\Delta_j t} + a_j^\dagger \sigma_- e^{-i\Delta_j t} \right), \tag{23}$$

with the detuning parameter  $\Delta_j$  given by

$$\Delta_j \equiv \Delta_j(n; \beta; \gamma) = \sum_k \Xi_k + \Xi(n; \beta; \gamma) - nv_j(\langle m_j \rangle; \beta), \tag{24}$$

and where the spin transition frequency  $\omega$  in Eq. (13) was thermally averaged over the  $2^n - 1$  configurations of the manifold contained in the unit operator of the Grassmann space after subtracting the norm of the vacuum state. Analytical details concerning the reduction of the  $n$ -spin model to a two-level system by including all the thermally averaged configurations of the excited states manifold is described in Refs. 40 and 41. It is further observed from Eq. (23) that

$$[\mathcal{V}_1(t), \mathcal{V}_2(t)] = \hbar^2 g_1 g_2 \sigma_z (a_1 a_2^\dagger e^{i(\Delta_1 - \Delta_2)t} - \text{h.c.}). \tag{25}$$

Thus, the non-vanishing of this commutator requires special care. Moreover, since in this model system  $\mathcal{H}_0$  does not commute with  $\mathcal{H}_1$ , except in the degenerate state  $\nu_1(\langle m_1 \rangle; \beta) = \nu_2(\langle m_2 \rangle; \beta)$  at the exact resonance with the spin transition frequency, the operators  $\mathcal{V}(t_1), \mathcal{V}(t_2), \dots$ , taken at different times  $t_1, t_2, \dots$  fail to commute. In fact, after some rather lengthy but straightforward algebra, the commutator  $[\mathcal{V}(t_1), \mathcal{V}(t_2)]$  is found to be

$$\begin{aligned} [\mathcal{V}(t_1), \mathcal{V}(t_2)] &= \sum_{i=1}^2 \sum_{j=1}^2 [\mathcal{V}_i(t_1), \mathcal{V}_j(t_2)] \\ &= \hbar^2 \left[ 2i \sum_{j=1}^2 g_j^2 (\sigma_+ \sigma_- + \sigma_z a_j^\dagger a_j) \sin[\Delta_j(t_1 - t_2)] \right. \\ &\quad \left. + g_1 g_2 \sigma_z (a_1 a_2^\dagger (e^{i(\Delta_1 t_1 - \Delta_2 t_2)} - e^{i(\Delta_1 t_2 - \Delta_2 t_1)}) - \text{h.c.}) \right], \tag{26} \end{aligned}$$

which clearly does not vanish, except in the (nontrivial) particular case of exact simultaneous resonance of both modes with the spin transition frequency. There are four cases of interest: (i)  $\Delta_1 = \Delta_2 = 0$ ; (ii)  $0 \neq \Delta_1 \neq \Delta_2 \neq 0$ ; (iii)  $\Delta_1 = \Delta_2 \neq 0$ ; (iv)  $\Delta_1 = 0; \Delta_2 \neq 0$ . These four cases will be separately investigated. The system dynamics will be examined through the density operator formalism.

### 3.1. Exact simultaneous resonance ( $\Delta_1 = \Delta_2 = 0$ )

In this case, the cavity field is doubly degenerate and exactly resonant with the spin transition frequency. The unitary time-evolution operator is given by

$$U(t) = \exp(-i/\hbar \mathcal{V}t), \tag{27}$$

where  $\mathcal{V}$  is given by Eq. (23) with  $\Delta_1 = \Delta_2 = 0$ , i.e.,

$$\mathcal{V} = \sum_{j=1}^2 g_j (\sigma_+ a_j + a_j^\dagger \sigma_-). \tag{28}$$



Introducing the *hermitian* operator  $A(a, a^\dagger)$  given by

$$A(a, a^\dagger) = \sum_{i=1}^2 \sum_{j=1}^2 g_i g_j a_i a_j^\dagger, \tag{29}$$

it is found that the even and odd powers of  $\mathcal{V}$  can be written as

$$\mathcal{V}^{2l} = \sqrt{A(a, a^\dagger)}^{2l} |b\rangle\langle b| + \sqrt{A^\dagger(a, a^\dagger)}^{2l} |a\rangle\langle a|, \tag{30}$$

$$\mathcal{V}^{2l+1} = \frac{\sqrt{A(a, a^\dagger)}^{2l+1}}{\sqrt{A(a, a^\dagger)}} \sum_{j=1}^2 g_j a_j |b\rangle\langle a| + \text{h.c.}, \tag{31}$$

where nilpotency and idempotency properties of  $\sigma_\pm$  and  $\sigma_\pm \sigma_\mp$  (i.e.,  $\sigma_\pm^k = 0, k \geq 2$ ;  $(\sigma_\pm \sigma_\mp)^k = \sigma_\pm \sigma_\mp, k \geq 1$ ) were used. Thus the unitary time-evolution operator in Eq. (27) becomes

$$U(t) = \cos\left(\sqrt{A(a, a^\dagger)} t\right) |b\rangle\langle b| + \cos\left(\sqrt{A^\dagger(a, a^\dagger)} t\right) |a\rangle\langle a| - i \left[ \frac{\sin\left(\sqrt{A(a, a^\dagger)} t\right)}{\sqrt{A(a, a^\dagger)}} \sum_{j=1}^2 g_j a_j |b\rangle\langle a| + \text{h.c.} \right]. \tag{32}$$

Since various dissipation processes in the interaction of light and matter are not included in the JCM, the dynamics of the JCM is not stationary, and depends on the initial conditions of the system and the cavity field. Thus, it is assumed that initially, the field modes are in coherent states  $|\alpha_1 \alpha_2\rangle$  and the spin system is in the excited state  $|b\rangle$ , i.e.,

$$|\psi(0)\rangle = |b; \alpha_1 \alpha_2\rangle = \sum_{m_1=0}^\infty \sum_{m_2=0}^\infty c_{m_1 m_2}(0) |b; m_1 m_2\rangle, \tag{33}$$

and the coefficients  $c_{m_1 m_2}(0)$  are given in terms of the density operator matrix elements  $\rho(0)$ . It is further assumed that at  $t = 0$ , the two modes have the same photon distribution,

$$\begin{aligned} \rho(0) &= |\psi(0)\rangle\langle\psi(0)| \\ &= \sum_{n_1=0}^\infty \sum_{n_2=0}^\infty \sum_{m_1=0}^\infty \sum_{m_2=0}^\infty c_{n_1}(0) c_{n_2}(0) c_{m_1}^*(0) c_{m_2}^*(0) |b; m_1 m_2\rangle\langle b; n_1 n_2|, \end{aligned} \tag{34}$$

that is,

$$c_{m_1 m_2}(0) = [\rho_{m_1 m_1}(0) \rho_{m_2 m_2}(0)]^{1/2}. \tag{35}$$

Various nonclassical effects in the JCM can be generated by choosing different initial states of the field. For example, when the cavity field is initially in a coherent state of photons, one finds that the level occupation probability of the system can display collapse and revivals<sup>2</sup> of the Rabi oscillations in a field that is not in a pure number state. This point is discussed in Subsect. 4.1.

The density operator at time  $t$  is obtained through the unitary time-evolution operator via

$$\rho(t) = |\psi(t)\rangle\langle\psi(t)| = U(t)\rho(0)U^\dagger(t), \tag{36}$$

where the time dependent wavefunction is given by

$$|\psi(t)\rangle = \sum_{n_1=0}^{\infty} \sum_{n_2=0}^{\infty} c_{n_1 n_2}(0)U(t)|b; n_1 n_2\rangle. \tag{37}$$

Thus, the probability amplitude for the ground state is obtained from

$$|c_{a; m_1 m_2}(t)| = \sqrt{\langle a; m_1 m_2 | U(t)\rho(0)U^\dagger(t) | a; m_1 m_2 \rangle}. \tag{38}$$

Up to this point, there are no approximations involved in the obtainment of this probability amplitude. In fact, the evolution operator in Eq. (32) is exact to all orders. However, to explicitly evaluate the matrix element  $\langle a; m_1 m_2 | U(t) | b; n_1 n_2 \rangle$  implicit in Eq. (38), it is convenient to *linearize* the expansion of  $A(a, a^\dagger)^l$  involved in Eq. (32) according to

$$A(a, a^\dagger)^l \rightarrow \sum_{i=1}^2 [g_i^2 a_i a_i^\dagger]^l + \text{highly non-linear cross terms}. \tag{39}$$

The higher-order cross terms in this equation involve powers of the bosonic operators  $a_j^p, a_k^{\dagger q}$  which can be evaluated through

$$a_j^p |n_j\rangle = \sqrt{\frac{n_j!}{(n_j - p)!}} |n_j - p\rangle, \tag{40}$$

$$a_k^{\dagger q} |n_k\rangle = \sqrt{\frac{(n_k + q)!}{n_k!}} |n_k + q\rangle, \tag{41}$$

with  $j, k = 1, 2$  and  $p \leq n_j$ . This rather complex possibility can be investigated via time dependent perturbation theory of the evolution operator using the Dyson expansion, as described in the next Subsections in the cases of off-resonant states (degenerate and nondegenerate states of the field modes) and exact resonance of a single mode. Here we neglect these higher-order cross terms, which amounts to keeping in the expansion of Eq. (29) only the diagonal terms, i.e., those terms with  $i = j$ . In this way, the double summation over  $n_1$  and  $n_2$  in Eq. (37) is restricted only to those terms involving the photon number operators  $n_i = a_i^\dagger a_i$ . This procedure then allows the time-evolution operator matrix element for the ground state to be written as

$$\langle a; m_1 m_2 | U(t) | b; n_1 n_2 \rangle = -i \sum_{j \neq k}^2 \frac{\sin(\chi_{n_j+1n_k}^{g_j g_k} t)}{\chi_{n_j+1n_k}^{g_j g_k}} g_j \sqrt{n_j + 1} \delta_{m_j n_j+1} \delta_{m_k n_k}, \tag{42}$$

with the function  $\chi_{m_1 m_2}^{g_1 g_2}$  defined by

$$\chi_{m_1 m_2}^{g_1 g_2} = \sqrt{\sum_{j=1}^2 g_j^2 m_j}. \tag{43}$$

Thus, the squared coefficient  $c_{a; m_1 m_2}(t)$  for the ground state can be written as

$$|c_{a; m_1 m_2}(t)|^2 = |\mathcal{F}_{m_1 m_2}^{g_1 g_2}(t)|^2 \left[ \sum_{j \neq k}^2 g_j \sqrt{m_j \rho_{m_j - 1 m_j - 1}(0) \rho_{m_k m_k}(0)} \right]^2, \tag{44}$$

where the time dependent fluctuation factor  $\mathcal{F}_{m_1 m_2}^{g_1 g_2}(t)$  is given by

$$\mathcal{F}_{m_1 m_2}^{g_1 g_2}(t) = \frac{\sin(\chi_{m_1 m_2}^{g_1 g_2} t)}{\chi_{m_1 m_2}^{g_1 g_2}}. \tag{45}$$

Likewise, contributions to the excited state  $|b\rangle$  are given by

$$\begin{aligned} c_{b; m_1 m_2}(t) &= \langle b; m_1 m_2 | \psi(t) \rangle \\ &= \sum_{n_1=0}^{\infty} \sum_{n_2=0}^{\infty} c_{n_1 n_2}(0) \langle b; m_1 m_2 | U(t) | b; n_1 n_2 \rangle, \end{aligned} \tag{46}$$

where the time-evolution operator matrix element  $\langle b; m_1 m_2 | U(t) | b; n_1 n_2 \rangle$  is given by

$$\begin{aligned} \langle b; m_1 m_2 | U(t) | b; n_1 n_2 \rangle &= \langle b; m_1 m_2 | \cos\left(\sqrt{A(a, a^\dagger)} t\right) | b; n_1 n_2 \rangle \\ &= \cos(\chi_{m_1+1 m_2+1}^{g_1 g_2} t) \delta_{m_1 n_1} \delta_{m_2 n_2}, \end{aligned} \tag{47}$$

and therefore the density operator diagonal matrix element associated with the excited state becomes

$$|c_{b; m_1 m_2}(t)|^2 = \rho_{m_1 m_1}(0) \rho_{m_2 m_2}(0) \cos^2(\chi_{m_1+1 m_2+1}^{g_1 g_2} t), \tag{48}$$

where the linearization (39) was used to evaluate the time-evolution operator matrix elements in Eq. (47).

### 3.2. Off-resonant states. Nondegenerate case ( $0 \neq \Delta_1 \neq \Delta_2 \neq 0$ )

We now deal with off-resonant states (this obviously corresponds to the nondegenerate case of the two modes of the field), i.e.,  $\Delta_j \neq 0$  with  $\Delta_1 \neq \Delta_2$ , and therefore the time-evolution operator in the interaction picture reads (Dyson expansion)

$$U_I(t) = \mathcal{F} \exp \left[ -\frac{i}{\hbar} \int_0^t \mathcal{V}(t) dt \right], \tag{49}$$

where  $\mathcal{F}$  is the time-ordering operator, which is a shorthand notation for the expansion

$$\begin{aligned} \mathcal{F} \exp \left[ -\frac{i}{\hbar} \int_0^t \mathcal{V}(t) dt \right] &= 1 - \frac{i}{\hbar} \int_0^t \mathcal{V}(t_1) dt_1 \\ &+ \left( -\frac{i}{\hbar} \right)^2 \int_0^t dt_1 \int_0^{t_1} dt_2 \mathcal{V}(t_1) \mathcal{V}(t_2) \\ &+ \left( -\frac{i}{\hbar} \right)^3 \int_0^t dt_1 \int_0^{t_1} dt_2 \int_0^{t_2} dt_3 \mathcal{V}(t_1) \mathcal{V}(t_2) \mathcal{V}(t_3) \\ &+ \dots \equiv \sum_{n=0}^{\infty} U_{In}(t). \end{aligned} \quad (50)$$

The different contributions to the interaction picture time evolution operator up to third-order are given by ( $U_{I0} = 1$ )

$$U_{I1}(t) = \sum_{j=1}^2 g_j (\sigma_+ a_j \phi_j(t) - a_j^\dagger \sigma_- \phi_j^*(t)), \quad (51)$$

$$U_{I2}(t) = \sum_{j=1}^2 \sum_{k=1}^2 g_j g_k (\sigma_+ a_j a_k^\dagger \sigma_- \phi_{jk}(t) + a_j^\dagger \sigma_- \sigma_+ a_k \phi_{jk}^*(t)), \quad (52)$$

$$U_{I3}(t) = \sum_{j=1}^2 \sum_{k=1}^2 \sum_{l=1}^2 g_j g_k g_l (\sigma_+ a_j a_k^\dagger \sigma_- \sigma_+ a_l \phi_{jkl}(t) - a_j^\dagger \sigma_- \sigma_+ a_k a_l^\dagger \sigma_- \phi_{jkl}^*(t)), \quad (53)$$

where the time dependent functions arising from the one-, two-, and three-times integrals in Eq. (50) are found to be given by ( $j, k = 1, 2; j \neq k$ )

$$\phi_j(t) = \frac{1 - e^{i\Delta_j t}}{\Delta_j}, \quad (54)$$

$$\phi_{jj}(t) = \frac{e^{i\Delta_j t} - 1 - it\Delta_j}{\Delta_j^2}, \quad (55)$$

$$\phi_{jk}(t) = \frac{e^{i\Delta_j t} - 1}{\Delta_j \Delta_k} - \frac{e^{i(\Delta_j - \Delta_k)t} - 1}{\Delta_k (\Delta_j - \Delta_k)}, \quad (56)$$

$$\phi_{jjj}(t) = \frac{2(e^{i\Delta_j t} - 1) - it\Delta_j(1 + e^{i\Delta_j t})}{\Delta_j^3}, \quad (57)$$

$$\phi_{jjk}(t) = \frac{e^{i\Delta_j t} - 1}{\Delta_j^2 (\Delta_k - \Delta_j)} + \frac{e^{i\Delta_k t} - 1}{\Delta_k^2 (\Delta_j - \Delta_k)} - \frac{it}{\Delta_j \Delta_k}, \quad (58)$$

$$\phi_{jkj}(t) = \frac{e^{i(2\Delta_j - \Delta_k)t} - 1}{\Delta_j (\Delta_k - \Delta_j) (2\Delta_j - \Delta_k)} + \frac{e^{i\Delta_j t} (e^{-i\Delta_k t} - 1)}{\Delta_j \Delta_k (\Delta_k - \Delta_j)}, \quad (59)$$

$$\phi_{jkk}(t) = \frac{e^{i\Delta_j t}(1 - it\Delta_j) - 1}{\Delta_j^2 \Delta_k} + \frac{e^{i\Delta_j t} - 1}{\Delta_j \Delta_k^2} + \frac{1 - e^{i(\Delta_j - \Delta_k)t}}{\Delta_k^2(\Delta_j - \Delta_k)}. \tag{60}$$

The interaction picture state vector at any time  $t$  is obtained from  $|\psi(0)\rangle$  via the unitary evolution operator  $U_I(t)$ ,

$$|\psi_I(t)\rangle = \sum_{n=0}^{\infty} \sum_{m_1=0}^{\infty} \sum_{m_2=0}^{\infty} c_{m_1 m_2}(0) U_{In}(t) |b; m_1 m_2\rangle. \tag{61}$$

In the present study, the different properties arising from an excited initial state and its decay to the ground state are to be computed through second- and third-order perturbation expansion for the excited and ground states respectively. Thus, up to second order, the non-vanishing time evolution operator diagonal matrix elements for the excited state are computed from

$$\langle b; n_1 n_2 | U_{I0} | b; m_1 m_2 \rangle = \delta_{n_1 m_1} \delta_{n_2 m_2}, \tag{62}$$

and

$$\begin{aligned} &\langle b; n_1 n_2 | U_{I2}(t) | b; m_1 m_2 \rangle \\ &= \sum_{j=1}^2 \sum_{k=1}^2 g_j g_k \phi_{jk}(t) \langle b; n_1 n_2 | \sigma_+ a_j a_k^\dagger \sigma_- | b; m_1 m_2 \rangle. \end{aligned} \tag{63}$$

Evaluation of this cavity matrix element through standard relations of bosonic operators and their associated Fock states yields

$$\begin{aligned} \langle b; n_1 n_2 | U_{I2}(t) | b; m_1 m_2 \rangle &= \sum_{j \neq k} (g_j^2 \phi_{jj}(t) (m_j + 1) \delta_{n_j m_j} \delta_{n_k m_k} \\ &+ g_j g_k \phi_{jk}(t) [m_j (m_k + 1)]^{1/2} \delta_{n_j m_j - 1} \delta_{n_k m_k + 1}). \end{aligned} \tag{64}$$

Thus, the probability amplitude  $c_{b; n_1 n_2}(t)$  for the excited state becomes

$$\begin{aligned} c_{b; n_1 n_2}(t) &= \langle b; n_1 n_2 | \psi_I(t) \rangle \\ &= \left( 1 + \sum_{j=1}^2 g_j^2 \phi_{jj}(t) (n_j + 1) \right) [\rho_{n_1 n_1}(0) \rho_{n_2 n_2}(0)]^{1/2} \\ &+ \sum_{j \neq k} g_j g_k \phi_{jk}(t) [n_k (n_j + 1)]^{1/2} [\rho_{n_j + 1 n_j + 1}(0) \rho_{n_k - 1 n_k - 1}(0)]^{1/2}. \end{aligned} \tag{65}$$

Likewise, projection onto  $\langle a; n_1 n_2 |$  yields the probability amplitude for the ground state as

$$c_{a; n_1 n_2}(t) = \sum_{m_1=0}^{\infty} \sum_{m_2=0}^{\infty} c_{m_1 m_2}(0) \langle a; n_1 n_2 | U_I(t) | b; m_1 m_2 \rangle, \tag{66}$$

which then requires evaluation of the time evolution operator off-diagonal matrix elements, given by

$$\begin{aligned} \langle a; n_1 n_2 | U_{I1}(t) | b; m_1 m_2 \rangle &= - \sum_{j=1}^2 g_j \phi_j^*(t) \langle a; n_1 n_2 | a_j^\dagger \sigma_- | b; m_1 m_2 \rangle \\ &= - \sum_{j \neq k}^2 g_j \phi_j^*(t) (m_j + 1)^{1/2} \delta_{n_j m_j + 1} \delta_{n_k m_k}, \end{aligned} \quad (67)$$

and

$$\begin{aligned} \langle a; n_1 n_2 | U_{I3}(t) | b; m_1 m_2 \rangle &= - \sum_{j=1}^2 \sum_{k=1}^2 \sum_{l=1}^2 g_j g_k g_l \phi_{jkl}^*(t) \langle a; n_1 n_2 | a_j^\dagger \sigma_- \sigma_+ a_k a_l^\dagger \sigma_- | b; m_1 m_2 \rangle, \end{aligned} \quad (68)$$

that is,

$$\begin{aligned} \langle a; n_1 n_2 | U_{I3}(t) | b; m_1 m_2 \rangle &= - \sum_{j \neq k}^2 [g_j^3 \phi_{jjj}^*(t) (m_j + 1)^{3/2} \delta_{n_j m_j + 1} \delta_{n_k m_k} \\ &\quad + g_j^2 g_k (\phi_{jjk}^*(t) m_j (m_k + 1)^{1/2} \delta_{n_j m_j} \delta_{n_k m_k + 1} \\ &\quad + \phi_{jkj}^*(t) [(m_j + 1)(m_j + 2)m_k]^{1/2} \delta_{n_j m_j + 2} \delta_{n_k m_k - 1} \\ &\quad + \phi_{jkk}^*(t) (m_k + 1)(m_j + 1)^{1/2} \delta_{n_j m_j + 1} \delta_{n_k m_k}], \end{aligned} \quad (69)$$

where standard relations of Fock states were used once more. Thus, up to third order, the probability amplitude  $c_{a;n_1 n_2}(t)$  for the ground state is obtained by substituting Eqs. (67) and (69) into Eq. (66) to yield

$$\begin{aligned} c_{a;n_1 n_2}(t) &= - \sum_{j \neq k}^2 [g_j \phi_j^*(t) n_j^{1/2} [\rho_{n_j - 1 n_j - 1}(0) \rho_{n_k n_k}(0)]^{1/2} \\ &\quad + g_j^3 \phi_{jjj}^*(t) n_j^{3/2} [\rho_{n_j - 1 n_j - 1}(0) \rho_{n_k n_k}(0)]^{1/2} \\ &\quad + g_j^2 g_k (\phi_{jjk}^*(t) n_j n_k^{1/2} [\rho_{n_j n_j}(0) \rho_{n_k - 1 n_k - 1}(0)]^{1/2} \\ &\quad + \phi_{jkj}^*(t) [(n_j - 1) n_j (n_k + 1)]^{1/2} [\rho_{n_j - 2 n_j - 2}(0) \rho_{n_k + 1 n_k + 1}(0)]^{1/2} \\ &\quad + \phi_{jkk}^*(t) n_j^{1/2} (n_k + 1) [\rho_{n_j - 1 n_j - 1}(0) \rho_{n_k n_k}(0)]^{1/2}]. \end{aligned} \quad (70)$$

At any time  $t$ , the state vector  $|\psi_I(t)\rangle$  is a linear combination of the states  $|b; n_1 n_2\rangle$  and  $|a; n_1 n_2\rangle$ . Here  $|b; n_1 n_2\rangle$  is the state in which the spin system is in the excited state  $|b\rangle$  and the field has  $n_1$  photons associated to the mode of frequency  $\nu_1$  and  $n_2$  photons associated to the mode of frequency  $\nu_2$ . A similar description exists for the ground state  $|a; n_1 n_2\rangle$ . As we are using the interaction picture, we use the slowly varying probability amplitudes  $c_{a;n_1 n_2}(t)$  and  $c_{b;n_1 n_2}(t)$ . The expressions

$|c_{b;n_1n_2}(t)|^2$  and  $|c_{a;n_1n_2}(t)|^2$  represent the probabilities that, at time  $t$ , the field has  $n_1$  photons of frequency  $\nu_1$ ,  $n_2$  photons of frequency  $\nu_2$  and the system is in levels  $|b\rangle$  and  $|a\rangle$ , respectively. The probability  $p(n_1, n_2)$  that there are  $n_1$  photons of frequency  $\nu_1$  and  $n_2$  photons of frequency  $\nu_2$  present simultaneously in the field at time  $t$  at a given temperature is therefore obtained by taking the trace over the spin states, i.e.,

$$\begin{aligned}
 p(n_1, n_2; t) &= \text{Tr } \rho_{n_1n_2}(t) = \rho_{n_1n_2}^{aa}(t) + \rho_{n_1n_2}^{bb}(t) \\
 &\equiv |c_{a;n_1n_2}(t)|^2 + |c_{b;n_1n_2}(t)|^2,
 \end{aligned}
 \tag{71}$$

where  $\text{Tr } \rho_{n_1n_2}(t)$  stands for the partial trace  $\text{Tr}_s \langle n_1n_2 | \rho(t) | n_1n_2 \rangle$  and  $\rho_{mm}(0)$  in Eqs. (65) and (70) is the probability that there are  $m$  photons present in the field at time  $t = 0$ , i.e.,  $\rho_{mm}(0) = |c_m(0)|^2$ .

**3.3. Off-resonant states. Degenerate case ( $\Delta_1 = \Delta_2 \neq 0$ )**

In this case, the field is doubly degenerate, but there is no resonance with the spin transition frequency. Setting  $\Delta_1 = \Delta_2$  in Eq. (23) and evaluating of the multiple time integrals in Eq. (50) leads to  $(j, k, l = 1, 2)$

$$\phi_{jk}(t) = \phi_{jj}(t),
 \tag{72}$$

$$\phi_{jkl}(t) = \phi_{jjj}(t),
 \tag{73}$$

where the time dependent functions  $\phi_{jj}(t)$  and  $\phi_{jjj}(t)$  are given by Eqs. (55) and (57). Thus, the time-evolution operator matrix elements for the excited and initial states and the associated probability amplitudes given in Eqs. (64)–(70) have to be evaluated using Eqs. (72) and (73).

**3.4. Exact resonance of one mode ( $\Delta_1 = 0; \Delta_2 \neq 0$ )**

In this case, there is a partial resonance of a single mode, but the other is associated to an off-resonant state. This nondegenerate particular case converts Eqs. (54)–(60) into

$$\phi_{11}(t) = -t^2/2!,
 \tag{74}$$

$$\phi_{12}(t) = \frac{e^{-i\Delta_2 t} + i\Delta_2 t - 1}{\Delta_2^2},
 \tag{75}$$

$$\phi_{21}(t) = \frac{e^{i\Delta_2 t}(i\Delta_2 t - 1) + 1}{\Delta_2^2},
 \tag{76}$$

$$\phi_{22}(t) = \frac{e^{i\Delta_2 t} - i\Delta_2 t - 1}{\Delta_2^2},
 \tag{77}$$

$$\phi_{111}(t) = it^3/3!,
 \tag{78}$$

$$\phi_{112}(t) = \frac{1 + i\Delta_2 t + (i\Delta_2 t)^2/2! - e^{i\Delta_2 t}}{\Delta_2^3}, \quad (79)$$

$$\phi_{121}(t) = \frac{2 - e^{-i\Delta_2 t}(2 + i\Delta_2 t) - i\Delta_2 t}{\Delta_2^3}, \quad (80)$$

$$\phi_{122}(t) = \frac{-1 + i\Delta_2 t - (i\Delta_2 t)^2/2! + e^{-i\Delta_2 t}}{\Delta_2^3}, \quad (81)$$

$$\phi_{211}(t) = \frac{e^{i\Delta_2 t}(-1 + i\Delta_2 t - (i\Delta_2 t)^2/2!) + 1}{\Delta_2^3}, \quad (82)$$

$$\phi_{212}(t) = \frac{e^{i\Delta_2 t}(2i\Delta_2 t - e^{i\Delta_2 t}) + 1}{2\Delta_2^3}, \quad (83)$$

$$\phi_{221}(t) = \frac{1 + i\Delta_2 t + (i\Delta_2 t)^2/2! - e^{i\Delta_2 t}}{\Delta_2^3}, \quad (84)$$

$$\phi_{222}(t) = \frac{2(e^{i\Delta_2 t} - 1) - i\Delta_2 t(1 + e^{i\Delta_2 t})}{\Delta_2^3}. \quad (85)$$

Thus, a set of time dependent probability amplitudes, from which the density operator matrix elements can be obtained, has been generated via truncation of the perturbative series of the time evolution operator. In this process, it was tacitly assumed that the interaction time is short. In fact, the short-time approximation approach is simple and enables us to explicitly derive short-time quantum statistics within the interaction time in a systematic way. Such analytic solutions provide information for more detailed computations, and make it possible to determine, in a straightforward way, all the possible states of light of the field exhibiting anticorrelation, antibunching, correlation bunching and full coherence. Computations of these nonclassical effects are discussed in the next Section.

#### 4. Results and Discussion

In the computations to be described below, a nearest-neighbor exchange coupling constant  $J = 4.31 \text{ cm}^{-1}$  was introduced in the Hamiltonian 2.1. The four cases described in Subsections 2.1-2.4 will be discussed. The antiperiodic boundary condition invoked in Sec. 2 to obtain the energy of the spin system restores the discrete translational invariance of the infinite lattice in the finite sample needed for the simulations.<sup>40-42,49</sup> The size of the spin chain is  $n = 14$ , and thus the manifold of excited states was thermally averaged over the 16383 configurations out of the vacuum state. In fact, the number of independent spin states of a given multiplicity, which exist for a system of  $n$  spins, denoted by  $f(n, S)$ , can be derived in an analogical fashion. The result is

$$f(n, S) = \frac{(2S + 1)n!}{(n/2 + S + 1)!(n/2 - S)!}, \quad (86)$$



Table 1. Number of Configurations of a given Multiplicity.

Multiplicity $2S + 1$	$f(n, S)$ $n = 14$
1	429
3	1001
5	1001
7	637
9	273
11	77
13	13
15	1

and the results are presented in Table 1 for  $n = 14$ . It is further observed that

$$\sum_S (2S + 1)f(n, S) = 2^n. \tag{87}$$

It is seen from the numbers given in Table 1 that Eq. (87) is indeed satisfied. This is consistent with the dimension of the trace of the unit operator in a basis of a Grassmann algebra.<sup>40–42,49,50</sup>

#### 4.1. Photon distribution and spin population inversion

Figure 1 displays the photon distribution in terms of  $\langle n_1 \rangle$  as given by Eq. (71) in the picosecond time scale  $t = 3.2$  ps in the case of exact simultaneous resonance of both modes, i.e., the trace over the spin states in Eq. (71) is calculated from Eqs. (44) and (48). It was assumed that the initial coherent state  $\rho_{m_i m_i}(0)$  is given

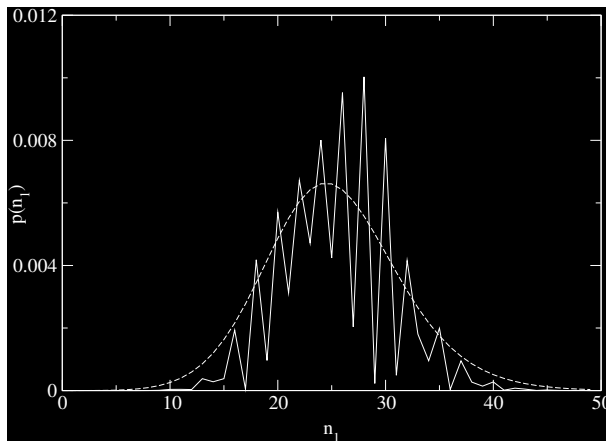


Fig. 1. Photon number distribution (solid curve) and its Laplace transform (dashed curve).  $\Delta_1 = \Delta_2 = 0$ ;  $\langle n_1 \rangle = \langle n_2 \rangle = 25$ ;  $g_1 = 158 \text{ cm}^{-1}$ ,  $g_2 = 5 \text{ cm}^{-1}$ . The initial coherent state of the field is given by a Poisson distribution.

by a Poisson distribution

$$\rho_{m_i m_i}(0) = \frac{\langle m_i \rangle^{m_i} e^{-\langle m_i \rangle}}{m_i!}. \tag{88}$$

A breakup at the photon distribution into a series of peaks (solid curve) can be seen. Also, for  $\langle n_1 \rangle \gg 1$ , the distribution is localized around  $\langle n_1 \rangle$ , and has a width  $(\Delta n_1)$  much narrower than that of  $\langle n_1 \rangle^{1/2}$ . One may think that the photon distribution in Eq. (71) is the result of a suitable mechanism for creating photon distributions of odd shapes, but we must remember that Eq. (71) is the result of the action of only one spin. To obtain a macroscopic change, one has to consider the influence of a large number of spins. These will then have some distribution in their parameter values that will smear the structure. To illustrate the statement, we assume the spins to have a distribution of the time they spend in the cavity. This is the case when any two levels involved in the manifold of excited states decay to a lower level with the rate  $\sigma$ . If this is the same at both levels, we can talk about the average lifetime  $\sigma^{-1}$  in the two states interacting with the radiation field. In radiative decay, the normalized distribution of the lifetime is  $\sigma \exp(-\sigma t)$ . The average photon distribution obtained when an ensemble of spins with this lifetime distribution has interacted with the two mode cavity field is then the Laplace transform of Eq. (71), where the coefficients  $c_{a;n_1 n_2}(t)$  and  $c_{b;n_1 n_2}(t)$  are given explicitly by Eqs. (44) and (48). Thus, for zero detuning of both modes and after some algebra, this process yields

$$\begin{aligned} \mathcal{L}\{\text{Tr } \rho(t)\} &= \sigma \int_0^\infty \text{Tr } \rho(t) e^{-\sigma t} dt \\ &= \frac{2}{G_{m_1 m_2}^{g_1 g_2}(\sigma)} \left[ \sum_{j \neq k}^2 g_j \sqrt{m_j \rho_{m_j-1 m_j-1}(0) \rho_{m_k m_k}(0)} \right]^2 \\ &\quad + \left( 1 - 2 \frac{[\chi_{m_1+1 m_2+1}^{g_1 g_2}]^2}{G_{m_1+1 m_2+1}^{g_1 g_2}(\sigma)} \right) \rho_{m_1 m_1}(0) \rho_{m_2 m_2}(0) \end{aligned} \tag{89}$$

with the function  $G_{m_1 m_2}^{g_1 g_2}(\sigma)$  defined as

$$G_{m_1 m_2}^{g_1 g_2}(\sigma) = 4[(\sigma/2)^2 + [\chi_{m_1 m_2}^{g_1 g_2}]^2]. \tag{90}$$

We can compare this distribution exemplified in Fig. 1, in which  $\sigma^{-1} = 3.2$  ps, with the photon distribution emerging from Eq. (71). The structure of the photon distribution (solid line) has been smeared out by the Laplace transform (dashed line), and the general shape is preserved.

As a first example of nontrivial nonclassical behavior in this model, we study the dynamics of the population inversion for the spin system initially in the excited state, interacting with the cavity field in an initial coherent state given by a

normalized Gaussian

$$\rho_{m_i, m_i}(0) = \frac{\exp[-(m_i - \langle m_i \rangle)^2 / 2\Gamma^2]}{\sum_{m_i} \exp[-(m_i - \langle m_i \rangle)^2 / 2\Gamma^2]}, \quad (91)$$

for the photon distribution function, with  $\Gamma = 4$ . The inversion is related to the probability amplitudes  $c_{b, n_1 n_2}(t)$  and  $c_{a, n_1 n_2}(t)$ , and is given by summing over  $n_1$  and  $n_2$  the difference of the squared coefficients. In terms of the density operator matrix elements, this process yields, with obvious notation

$$W(t) = \text{Tr } \rho_{n_1 n_2}(t) \sigma_z = \sum_{n_1=0}^{\infty} \sum_{n_2=0}^{\infty} [\text{Tr } \rho_{n_1 n_2}(t) - 2\rho_{n_1 n_2}^{aa}(t)]. \quad (92)$$

As a specific example, Fig. 2(a) shows this population inversion computed in the anisotropic limit  $\gamma = 1$  in the picosecond time scale and with  $\beta = 0.0001$ . This case corresponds to an off-resonant state of both modes, with the detuning parameters given by  $|\Delta_1| = 2585 \text{ cm}^{-1}$ ,  $|\Delta_2| = 2755 \text{ cm}^{-1}$ , and where the coefficients in Eq. (92) have to be consequently computed from Eqs. (65) and (70). 44 terms were included for each mode in the double summation of Eq. (90), i.e., 1936 terms in all. As expected, a time record resembling that for the usual Jaynes-Cummings standard model can be observed. It can also be observed that the minima become less deep with the passage of time before they approach the asymptotic limit of the envelopes and later, the minima decrease in the same magnitude. This behavior is repeated periodically with a period of 1.25 ps.

We can also compute the state of the system when the spins leave the cavity. This device prepares spins in a specific state, depending on the time they spend in the cavity. Taking the trace over the spin variables, this procedure yields, for the real and imaginary parts of the density operator off-diagonal matrix elements,

$$\begin{aligned} \frac{1}{2} [\rho^{ab}(t) + \rho^{ba}(t)] &\equiv \frac{1}{2} \sum_{n_1=0}^{\infty} \sum_{n_2=0}^{\infty} [\rho_{n_1 n_2}^{ab}(t) + \rho_{n_1 n_2}^{ba}(t)] \\ &= \cos(\phi_a - \phi_b) \sum_{n_1=0}^{\infty} \sum_{n_2=0}^{\infty} \sqrt{\rho_{n_1 n_2}^{aa}(t) \rho_{n_1 n_2}^{bb}(t)}, \end{aligned} \quad (93)$$

$$\begin{aligned} \frac{1}{2i} [\rho^{ab}(t) - \rho^{ba}(t)] &\equiv \frac{1}{2i} \sum_{n_1=0}^{\infty} \sum_{n_2=0}^{\infty} [\rho_{n_1 n_2}^{ab}(t) - \rho_{n_1 n_2}^{ba}(t)] \\ &= \sin(\phi_a - \phi_b) \sum_{n_1=0}^{\infty} \sum_{n_2=0}^{\infty} \sqrt{\rho_{n_1 n_2}^{bb}(t) \rho_{n_1 n_2}^{aa}(t)}, \end{aligned} \quad (94)$$

where  $\phi_a$  and  $\phi_b$  are the phases of the probability amplitudes associated to the states  $|a\rangle$  and  $|b\rangle$  respectively. It is clear that the dynamics is modulated by oscillatory factors involving the phase difference  $\phi_a - \phi_b$ . Figures 2(b) and 2(c) represent the oscillations of the real and imaginary parts of the density operator off-diagonal matrix elements as a function of time using the same set of parameters in Fig. 2(a).

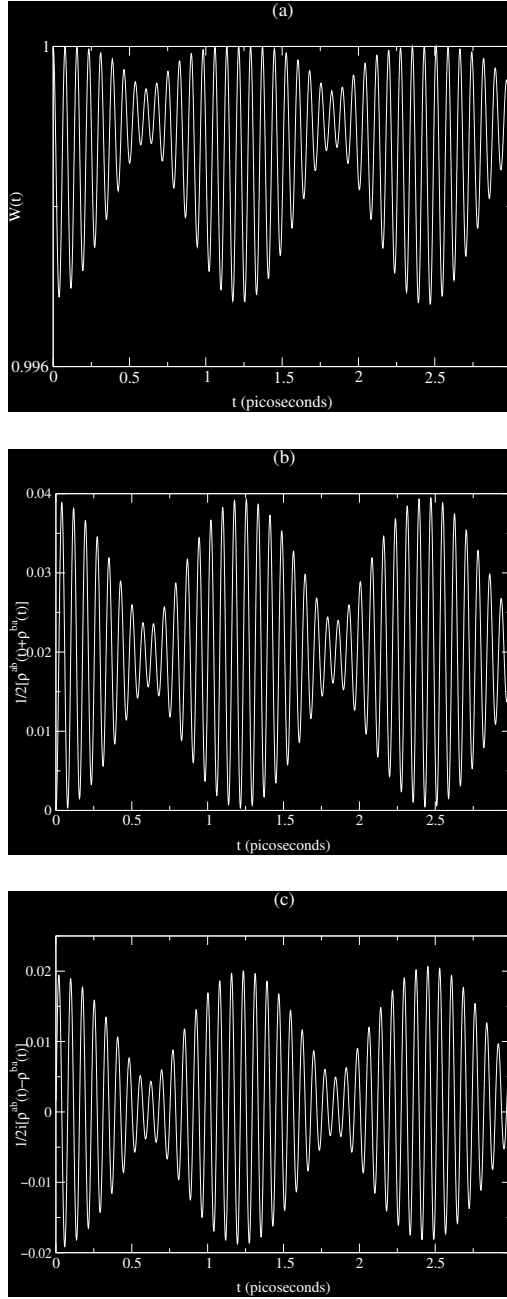


Fig. 2. Time evolution of the spin population inversion. (a)  $0 \neq \Delta_1 \neq \Delta_2 \neq 0$ ;  $\langle n_1 \rangle = 16$ ,  $\langle n_2 \rangle = 15$ ;  $g_1 = 5 \text{ cm}^{-1}$ ,  $g_2 = 8.3 \text{ cm}^{-1}$ . The initial coherent state of the field is given by a Gaussian distribution; (b) same as (a), but for the real part of the nondiagonal matrix elements of  $\rho(t)$ ; (c) same as (a) but for the imaginary part of the nondiagonal matrix elements of  $\rho(t)$ ; (d)  $\Delta_1 = \Delta_2 = 0$ ;  $\langle n_1 \rangle = \langle n_2 \rangle = 25$ . The initial coherent state of the field,  $\rho_{mm}(0)$ , is given by a Gaussian distribution.

In both figures, the envelope of the revivals is almost a Gaussian. The field is seen to equalize the populations rapidly within a time approximately of the order  $0.1/\sqrt{\langle n_1 \rangle g_1^2 + \langle n_2 \rangle g_2^2} = 0.088$  ps and later, the spin coherence causes oscillations, which are found near the time when the populations oscillate [cf. Fig. 2(a)], which is physically understandable. The field is essentially stationary. Its coherence is completely destroyed as the field amplitudes collapse, but is partially restored during revival periods. Thus, a more complete description of the pattern in Figs. 2(a)–2(c) follows from the computation of the population inversion in the limit of exact simultaneous resonance of both modes with the spin transition frequency,  $\Delta_1 = \Delta_2 = 0$ , as shown in Fig. 2(d). In this case, the dynamics involved in Eq. (92) was performed with the time dependent coefficients given by Eqs. (44) and (48), assuming a Gaussian distribution with  $\Gamma = 4$ . If the coupling constant of one mode (in this case the first mode) is large (solid line), as the time increases, the neighboring revivals increasingly overlap. In the overlap region, the Rabi oscillations are a result of the superposition of the oscillations from different overlapping revivals. For long times, therefore, when the overlap occurs between increasingly more revivals, the oscillations are then due to the superposition of many frequencies, and  $W(t)$  exhibits an apparently chaotic behavior. In fact, one can see that in the resonant case, the revivals are not well-separated in the long time regime and in fact, the inversion behaves in a fairly irregular manner. In the off-resonant case, however, the very regular and distinct revivals with the small amplitude appear. This discussion on the pattern of Figs. 2(a)–2(d) can be generalized as follows. Each term in the double summation of Eq. (92) represents Rabi oscillations for definite values of  $n_1, n_2$ . The photon distribution function  $\rho_{m_i, m_i}(0)$  determines the relative weight for each set of values of  $n_1, n_2$ . At the initial time,  $t = 0$ , the spin system is prepared in a definite state; thus all the terms in the double summation in Eq. (92) are correlated. As the time increases, the oscillations associated with different excitations have different frequencies, and therefore become uncorrelated, leading to a collapse of inversion. As the time is increased further, the correlation is restored and revival occurs. This behavior continues, and an infinite sequence of revivals is obtained. These revivals occur only because of the granular structure of the photon distribution, i.e., they are a manifestation of the quantum nature of the electromagnetic field, which is mathematically reflected in the discrete double summation. The collapses, on the other hand, occur because the many different components in the summation become out of phase. This structure is very similar to that found in the nonlinear Jaynes-Cummings model discussed in Ref. 34, where the interaction of essentially a two-level atom interacting with a two-mode radiation field through a Raman interaction is discussed through the use of a phenomenological Hamiltonian.

#### 4.2. Field statistics

We now study the dynamics of the field statistics of our system, with particular emphasis on the production of states of the field exhibiting nonclassical properties.

In particular, we examine the possible production of antibunched light, anticorrelations between the two modes, and possible violation of the Cauchy-Schwartz inequality.

But first, let us consider the time evolution of the average photon number in each mode. From Eq. (71) which gives the two-mode photon number distribution function, the average photon numbers  $\bar{n}_1(t)$ ,  $\bar{n}_2(t)$  are obtained as ( $i = 1, 2$ )

$$\bar{n}_i(t) = \text{Tr } \rho_{n_1 n_2}(t) a_i^\dagger a_i = \sum_{n_1=0}^{\infty} \sum_{n_2=0}^{\infty} n_i p(n_1, n_2; t), \quad (95)$$

and where  $\bar{n}_i(0) \equiv \langle n_i \rangle$ . The oscillations of the average photon numbers are clearly related to the Rabi oscillations, as seen in the spin inversion. Figures 3(a)–3(c) present the time evolution of  $\langle n_i \rangle$ , where it is clear that, as expected, these quantities exhibit the same pattern of collapse and revival as the spin inversion. In Fig. 3(a), the initial coherent state of the field is given by the Poisson distribution of Eq. (88), and corresponds to the case of exact simultaneous resonance. Figure 3(b) shows the time evolution when only the first mode is resonant (nondegenerate case), that is, the coefficients  $c_{b;n_1 n_2}(t)$ ,  $c_{a;n_1 n_2}(t)$  for the excited and ground states respectively, are computed via the time dependent functions given in Eqs. (74)–(85). The computation in this figure was conducted in the anisotropic limit  $\gamma = 1$ , with  $\Delta_2 = 31 \text{ cm}^{-1}$ , at a rather low temperature  $\beta = 10$ . The initial coherent state of the field was assumed to be given by the Gaussian distribution of Eq. (91) with the width  $\Gamma = 4$ . Similar computations in off-resonant states for the particular case  $\Delta_i = 32 \text{ cm}^{-1}$  ( $i = 1, 2$ ) are shown in Fig. 3(c) (degenerate case) with  $\gamma = 0$ ,  $\beta = 1$ , and the initial coherent state of the field is given by a Poisson distribution. In this case, the density operator matrix elements involved in the photon distribution  $p(n_1, n_2; t)$  have to be computed via Eqs. (72) and (73). It should be addressed that the results presented in Figs. 3(a)–3(c) are very similar to those given in Ref. 34 in connection with the dynamics of a Raman coupled model interacting with two quantized cavity fields. In Fig. 3(a), it is observed that the maximum amplitude of the modulation of  $\langle n(t) \rangle$  is unity, which simply reflects the fact that the spin system absorbs and emits only a single photon. If we allow detuning from the partially off-resonant states as in Figs. 3(b) and 3(c), then the apparently dissimilar behavior observed in these figures in comparison with Fig. 3(a) can be mainly attributed to the overlapping and washing out of consecutive revivals, which is due to the incommensurate nature of the single-photon coupling energies. If the JCM is extended to include two-photon coupling, then the possibility for commensurate energies arises.<sup>39</sup> The presence of detuning essentially changes the time scale such that the duration of every collapse and revival is lengthened.

We now turn to the problem of obtaining evidence of nonclassical properties of the light beams for which experimental evidence has recently been reported in the case of single-photon detection rates.<sup>52,53</sup> It is an important phenomenon in view of the possibility of generating highly nonclassical  $n$ -photon polarization states by superbunching effects associated with the bosonic nature of photons,<sup>54</sup> and also for characterizing the nonclassical nature of conditionally prepared single photons.<sup>55</sup>

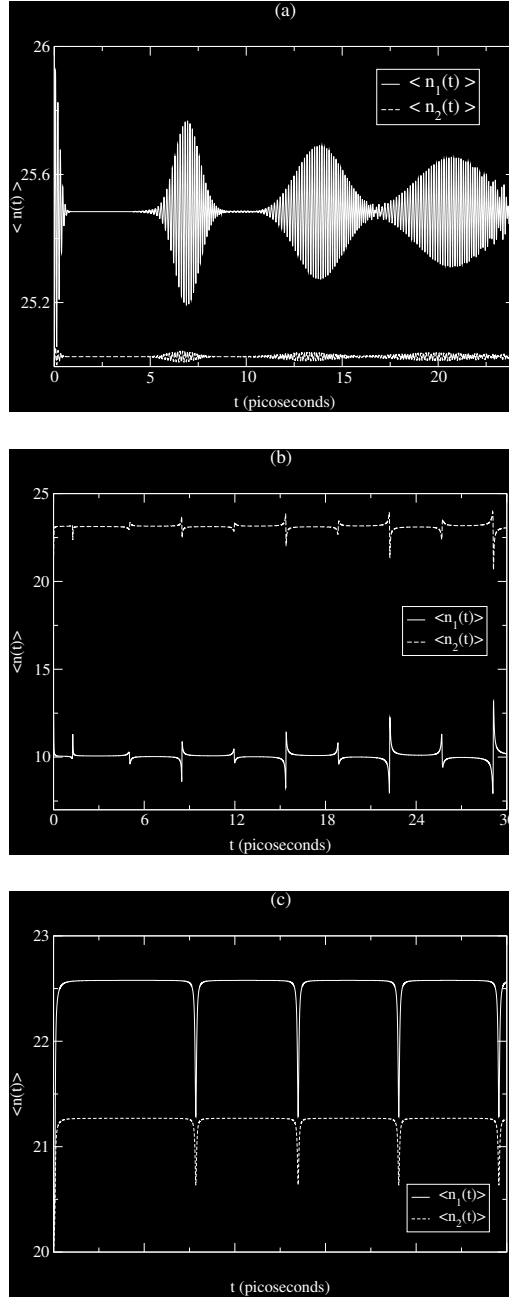


Fig. 3. Time evolution of the average photon number in each mode. (a)  $\Delta_1 = \Delta_2 = 0$ ;  $\langle n_1 \rangle = \langle n_2 \rangle = 25$ ;  $g_1 = 158 \text{ cm}^{-1}$ ,  $g_2 = 5 \text{ cm}^{-1}$ . The initial coherent state of the field,  $\rho_{mm}(0)$ , is given by a Poisson distribution; (b)  $\Delta_1 = 0$ ,  $\Delta_2 \neq 0$ ;  $\langle n_1 \rangle = 10$ ,  $\langle n_2 \rangle = 20$ ;  $g_1 = 25 \text{ cm}^{-1}$ ,  $g_2 = 105 \text{ cm}^{-1}$ . The initial coherent state of the field is given by a Gaussian distribution; (c)  $\Delta_1 = \Delta_2 \neq 0$ ;  $\langle n_1 \rangle = \langle n_2 \rangle = 20$ ;  $g_1 = 83 \text{ cm}^{-1}$ ,  $g_2 = 42 \text{ cm}^{-1}$ . The initial coherent state of the field is given by a Poisson distribution.

To characterize the statistical properties of the light beams, we introduce the function

$$\gamma_{ij}^{(2)} = \frac{\langle a_i^\dagger a_j^\dagger a_j a_i \rangle}{\langle a_i^\dagger a_i \rangle \langle a_j^\dagger a_j \rangle} \quad i, j = 1, 2. \tag{96}$$

Here  $\gamma_{ii}^{(2)}$  defines the degrees of second-order coherence in the modes and  $\gamma_{12}^{(2)}$  describes the degree of intermode correlation.

We first consider the second-order coherence of the modes. The function  $\gamma_{ii}^{(2)}$  can be written in terms of the normally ordered photon number variance  $\langle : (\Delta N_i)^2 : \rangle$  as

$$\gamma_{ii}^{(2)} = 1 + \frac{\langle : (\Delta N_i)^2 : \rangle}{\langle N_i \rangle^2}, \tag{97}$$

where  $N_i = a_i^\dagger a_i$  and

$$\langle : (\Delta N_i)^2 : \rangle = \langle a_i^\dagger a_i^\dagger a_i a_i \rangle - \langle N_i \rangle^2. \tag{98}$$

The light is nonclassical, exhibiting the sub-Poisson statistics, whenever  $\gamma_{ii}^{(2)} < 1$  or equivalently whenever  $\langle : (\Delta N_i)^2 : \rangle < 0$ . Since we are actually calculating the zero time delay coherence function, the states satisfying these conditions are more properly referred to as antibunched. The expectation values  $\langle N_i(t) \rangle = \bar{n}_i(t)$  are just those given by Eq. (95), while the first term on the right of Eq. (98) is given by

$$\langle a_i^\dagger(t) a_i^\dagger(t) a_i(t) a_i(t) \rangle = \sum_{n_1=0}^{\infty} \sum_{n_2=0}^{\infty} n_i(n_i - 1) p(n_1, n_2; t). \tag{99}$$

In Figs. 4(a) and 4(b), we plot the normally ordered variances for the first and second mode in the limit of exact simultaneous resonance of both modes  $\Delta_1 = \Delta_2 = 0$ . In this case, the dynamics is governed by the coefficients given in Eqs. (44) and (48), assuming in both cases that the initial coherent field is given by a Poisson distribution. We notice that both modes are bunched and antibunched. The collapse and revival patterns are of course the same as that for the spin inversion. However, as shown in Figs. 4(c) and 4(d), the use of the Gaussian distribution for the initial coherent state of the field with  $\Gamma = 4$  leads to antibunching for both modes with the collapse and revival patterns being the same as for the spin inversion.

Figures 5(a) and 5(b) show a comparison of the normally ordered variances of the photon number operators of both modes. The parameters used in Fig. 5(a) are the same as those used in Fig. 3(b), and a Gaussian distribution was assumed for the initial coherent state of the field. In Fig. 5(a),  $\Delta_1 = 0$  and  $\Delta_2 \neq 0$ . It is observed that no antibunching is present in the first mode, but it dominates the second mode. The parameters used in Fig. 5(b) are the same as those used in Fig. 3(c) and a Poisson distribution was assumed for the initial coherent state of the field. The computation in this figure corresponds to the doubly degenerate field in an off-resonant state with the spin system, i.e.,  $\Delta_1 = \Delta_2 \neq 0$ , and it is observed that



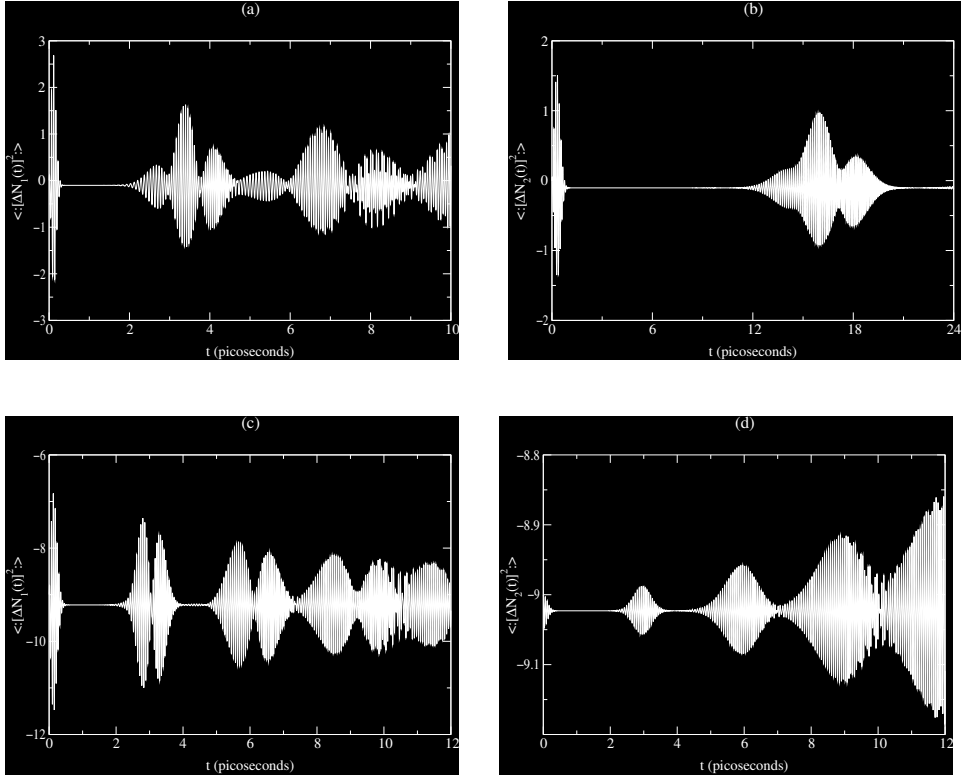


Fig. 4. Normally ordered variances for both modes. (a)  $\Delta_1 = \Delta_2 = 0$ ;  $\langle n_1 \rangle = \langle n_2 \rangle = 10$ ;  $g_1 = 478 \text{ cm}^{-1}$ ,  $g_2 = 338 \text{ cm}^{-1}$ . The initial coherent state of the field is given by a Poisson distribution; (b) same as (a) but for  $\langle n_1 \rangle = \langle n_2 \rangle = 25$ ;  $g_1 = 158 \text{ cm}^{-1}$ ,  $g_2 = 112 \text{ cm}^{-1}$ ; (c) same as (a) but for  $\langle n_1 \rangle = \langle n_2 \rangle = 25$ ;  $g_1 = 358 \text{ cm}^{-1}$ ,  $g_2 = 25 \text{ cm}^{-1}$  and the initial coherent state of the field is given by a Gaussian distribution; (d) same as (c).

both modes show antibunching. Apparently, for non-zero detuning as in Figs. 5(a) and 5(b), the sub-Poissonian statistics are present only for coupling constants larger than a certain cutoff, in the present case for  $g_i > 25 \text{ cm}^{-1}$ . The transition from antibunching to bunching in cavity QED was recently investigated experimentally in the context of photon statistics of the light emitted from an atomic ensemble into a single field mode of an optical cavity.<sup>16</sup>

The numerical results displayed in Figs. 5(a) and 5(b) show that, just as expected, the cavity will smear the amplitudes of the variances and spread the width of the revivals. This is because the revivals have dependences on the discrete nature of the photon-number distribution, which can be considered as the weighting factors of a discrete spectrum of Rabi frequencies. These are the reasons why the whole system in this case can be considered overdamped, and shows no Rabi oscillations; i.e., the reabsorption of emitted photons and the cavity-mediated interaction between different spins are both negligible.

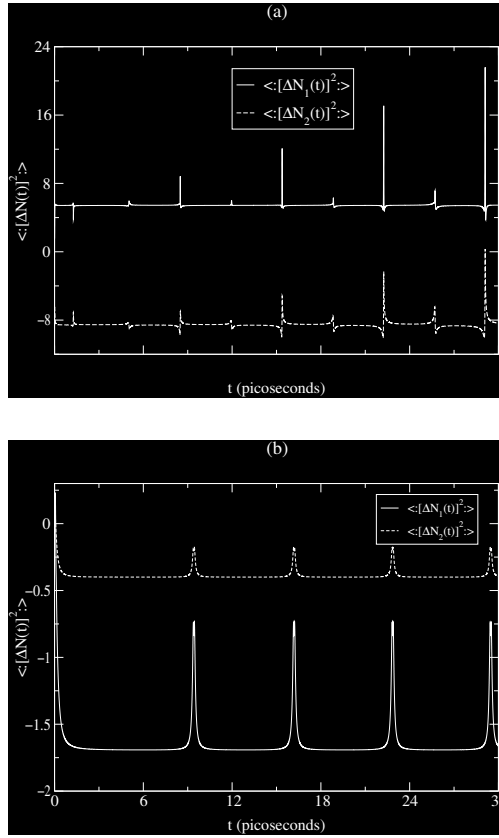


Fig. 5. Comparison of the normally ordered variances of the photon number operators of both modes. (a)  $\Delta_1 = 0, \Delta_2 \neq 0; \langle n_1 \rangle = 10, \langle n_2 \rangle = 20; g_1 = 25 \text{ cm}^{-1}, g_2 = 105 \text{ cm}^{-1}$  The initial coherent state of the field is given by a Gaussian distribution; (b) same as (a) but with  $\Delta_1 = \Delta_2 \neq 0; \langle n_1 \rangle = \langle n_2 \rangle = 20; g_1 = 83 \text{ cm}^{-1}, g_2 = 42 \text{ cm}^{-1}$  and the initial coherent state of the field is given by a Poisson distribution.

Also of interest is the degree of interbeam second-order coherence determined by

$$\gamma_{12}^{(2)} = \frac{\langle a_1^\dagger a_2^\dagger a_2 a_1 \rangle}{\langle a_1^\dagger a_1 \rangle \langle a_2^\dagger a_2 \rangle}, \tag{100}$$

recently discussed by Xiong *et al.*<sup>56</sup> We actually calculate the cross-correlation function (or the covariance of the product of the photon number operators) between the two modes as defined by

$$C(t) = \langle a_1^\dagger(t) a_2^\dagger(t) a_2(t) a_1(t) \rangle - \langle a_1^\dagger(t) a_1(t) \rangle \langle a_2^\dagger(t) a_2(t) \rangle, \tag{101}$$

which is proportional to the excess coincidence counting rate for a Hanbury-Brown-

Twiss-type experiment with two beams, where

$$\langle a_1^\dagger(t)a_2^\dagger(t)a_2(t)a_1(t) \rangle = \sum_{n_1=0}^{\infty} \sum_{n_2=0}^{\infty} n_1 n_2 p(n_1, n_2; t). \tag{102}$$

For  $C(t) = 0$ , the beams are uncorrelated ( $\gamma_{12}^{(2)} = 0$ ), for  $C(t) > 0$  they are correlated ( $\gamma_{12}^{(2)} > 0$ ), and for  $C(t) < 0$  they are anticorrelated ( $\gamma_{12}^{(2)} < 0$ ). The present model is similar in various aspects to the model introduced in Ref. 34 in which the net gain or loss of photons is zero, i.e., a zero-photon process. In such a model, where one photon is subtracted from one mode and added to the other, it should be expected that the two modes are predominantly anticorrelated. This is evident in Figs. 6(a)–6(c), which present the variation of  $C(t)$  versus  $t$  using a Poisson distribution for the initial coherent state of the field [Figs. 6(a) and 6(c)] and a Gaussian distribution with the width  $\Gamma = 5$  in Fig. 6(b).

Other than the nonclassical effects derived from the statistics of the field is the possible violation of the Cauchy-Schwartz inequality demonstrated experimentally in quantum noise-correlated light beams.<sup>47</sup> It reads

$$(\gamma_{12}^{(2)})^2 \leq \gamma_{11}^{(2)} \gamma_{22}^{(2)}, \tag{103}$$

which is violated by nonclassical states, indicating a nonclassical correlation between the beams. It is associated with the nonclassical correlation phenomenon between the two beams, and is associated with the nonexistence of a positive Glauber-Sudarshan P-representation.<sup>57</sup> We actually calculate the quantity

$$V(t) = \langle a_1^\dagger(t)a_2^\dagger(t)a_2(t)a_1(t) \rangle^2 - \langle a_1^\dagger(t)a_1^\dagger(t)a_1(t)a_1(t) \rangle \langle a_2^\dagger(t)a_2^\dagger(t)a_2(t)a_2(t) \rangle. \tag{104}$$

With these results, we calculate the time evolution of  $V(t)$  for zero detuning. Whenever  $V(t)$  is positive, the inequality in Eq. (103) is violated. This is evident in Fig. 7(a) for short discrete time periods and where a Poisson distribution was assumed for the initial coherent state of the field. As time increases, there are oscillations to both positive and negative values during the revivals while remaining at  $V(t) \simeq 0$  at other times. Thus, the mean value of the oscillations continues dropping below near zero to approach the steady state. In Fig. 7(b), there is no violation at all and  $V(t)$  is always negative, indicating that the field statistics become more classical as a result of the interaction with this single photon generalized JCM. This result is perhaps a little surprising since the form of the interaction would seem to preserve the correlations. In this computation, the initial coherent state of the field is described by a Gaussian distribution with  $\Gamma = 4$ . The dissimilar behavior in the nature of the time evolution in Figs. 7(a) and 7(b) reveals that in both cases,  $V(t)$  is strongly affected by the photon distribution function used to represent the initial coherence of the field. The Poisson distribution is more physical in the sense that this is the distribution followed by photons in a coherent state. This is probably

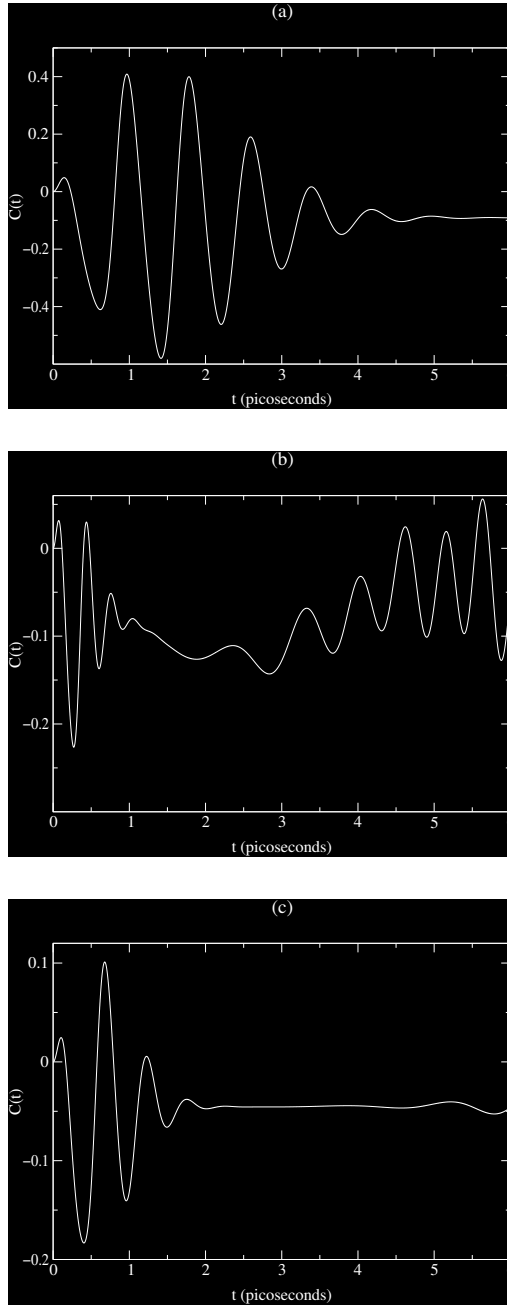


Fig. 6. Interbeam second-order coherence. (a)  $\Delta_1 = \Delta_2 = 0$ ;  $\langle n_1 \rangle = \langle n_2 \rangle = 25$ ;  $g_1 = 25 \text{ cm}^{-1}$ ,  $g_2 = 5 \text{ cm}^{-1}$ . The initial coherent state of the field is given by a Poisson distribution; (b) same as (a) but with  $\langle n_1 \rangle = \langle n_2 \rangle = 10$ ;  $g_1 = 92 \text{ cm}^{-1}$ ,  $g_2 = 5 \text{ cm}^{-1}$ ; and the initial coherent state of the field is given by a Gaussian distribution; (c) same as (a) but with  $\langle n_1 \rangle = \langle n_2 \rangle = 10$ ;  $g_1 = 58 \text{ cm}^{-1}$ ,  $g_2 = 5 \text{ cm}^{-1}$ . The initial coherent state of the field is given by a Poisson distribution.

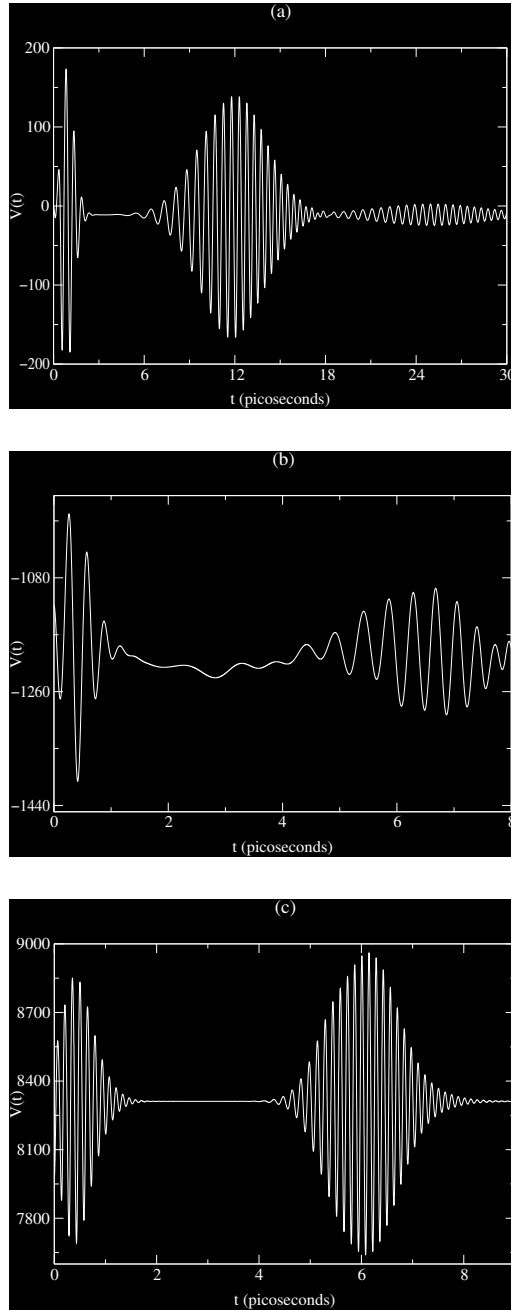


Fig. 7.  $V(t)$  versus  $t$  for  $\Delta_1 = \Delta_2 = 0$ . (a)  $\langle n_1 \rangle = \langle n_2 \rangle = 10$ ;  $g_1 = 58 \text{ cm}^{-1}$ ,  $g_2 = 17 \text{ cm}^{-1}$ . The initial coherent state of the field is given by a Poisson distribution; (b) same as (a) but with  $\langle n_1 \rangle = \langle n_2 \rangle = 10$ ;  $g_1 = 92 \text{ cm}^{-1}$ ,  $g_2 = 5 \text{ cm}^{-1}$ ; and the initial coherent state of the field is given by a Gaussian distribution; (c) same as (a) but with  $\langle n_1 \rangle = \langle n_2 \rangle = 25$ ;  $g_1 = 158 \text{ cm}^{-1}$ ,  $g_2 = 50 \text{ cm}^{-1}$  and the initial coherent state of the field is given by a photon distribution function.

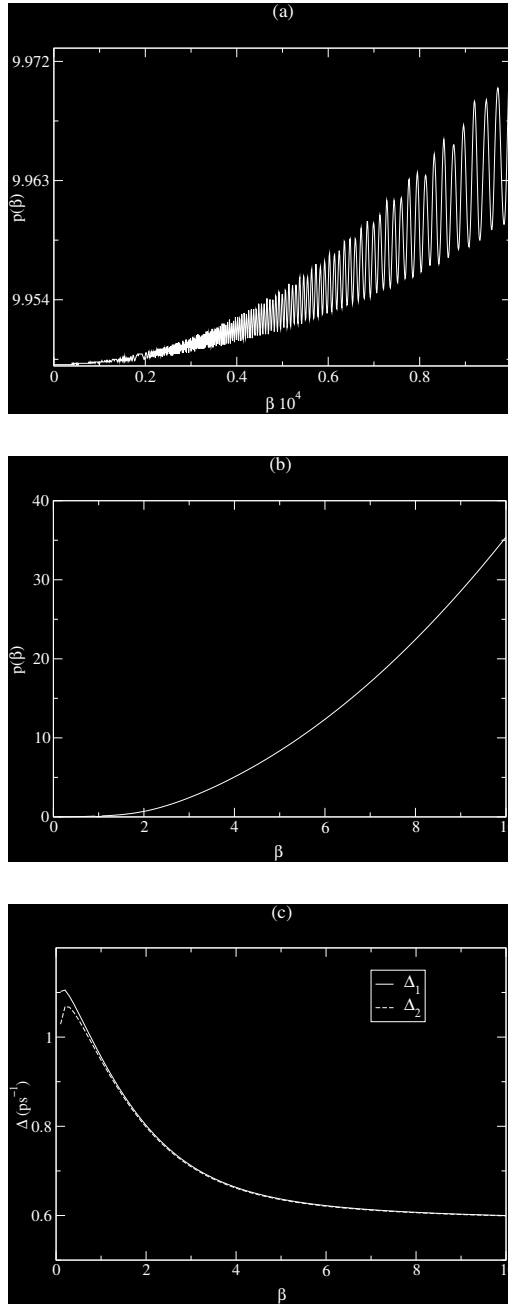


Fig. 8. Variation of the photon number distribution with the temperature in off-resonant states  $0 \neq \Delta_1 \neq \Delta_2 \neq 0$ ;  $\langle n_1 \rangle = 25$ ,  $\langle n_2 \rangle = 10$ ;  $g_1 = 5 \text{ cm}^{-1}$ ,  $g_2 = 8.3 \text{ cm}^{-1}$ . The initial coherent state of the field is given by a Poisson distribution. (a) Regime of very low  $\beta$ ; (b) same as (a) but in the regime of high  $\beta$ ; (c) Variation of the detuning parameters  $\Delta_1$ ,  $\Delta_2$  with the temperature in the regime of high  $\beta$ .

the reason for the violation observed in Fig. 7(a). In Fig. 7(c), where a photon distribution function for the field, initially in a two-photon coherent state is used, the inequality in Eq. (103) is always violated in this case. As is well-known, these states can be generated in a two-photon process, and are squeezed.<sup>58</sup> The photon-number distribution function for such a state is given by

$$\rho_{mm}(0) = \frac{(\tanh r)^m}{2^m m! \cosh r} \exp \left[ -|\chi|^2 + \frac{1}{2} [e^{-i\theta} \chi^2 + e^{i\theta} (\chi^*)^2] \tanh r \right] \times \left| H_m \left( \frac{\chi e^{-\theta/2}}{\sqrt{2} \cosh r \sinh r} \right) \right|^2, \tag{105}$$

where  $H_m(z)$  is the  $m$ th Hermite polynomial,  $r$  is the input squeeze parameter, and  $\chi$  is a dimensionless intensity parameter  $\chi = |\chi|e^{i\phi}$ . The direction of the coherent excitation is  $\phi$ , and  $\theta$  is the squeeze direction relative to that of coherent excitation. For simplicity, we take  $\phi = \theta/2$ . This figure shows the squeezing behavior for the small input squeezing  $r = 0.6$  and  $|\chi|^2 = 60$ .

To conclude, it is interesting to examine the behavior of the temperature distribution for a fixed mean number of photons in each mode. This is done in the limit of low and high  $\beta$  in Figs. 8(a) and 8(b) in the isotropic limit  $\gamma = 0$ , and for an initial coherent state of the field given by a Poisson distribution. It is observed that the excited and ground states are described by two completely different regimes. The limit of high temperatures characterizing the manifold of excited states becomes chaotic with rapid oscillations [Fig. 8(a)]. For larger values of  $\beta$ , this chaotic pattern is replaced, as expected, by a smooth behavior [Fig. 8(b)] characterizing the ground state. This should correspond to some asymptotic limit characterizing the vacuum state where all spins are ordered. This is clearly seen in Fig. 8(c), where the variations of the detuning parameters show an asymptotic behavior for high  $\beta$  characterizing the vacuum state. It is further observed that both detuning parameters show the same behavior. In fact, from Eqs. (14) and (24), it follows

$$\Delta_2 - \Delta_1 = \frac{1}{\hbar\beta} \ln \left( \frac{\langle m_2 \rangle (1 + \langle m_1 \rangle)}{\langle m_1 \rangle (1 + \langle m_2 \rangle)} \right), \tag{106}$$

an expression which becomes insensitive to the variation of  $\beta$  if both  $\langle m_i \rangle \gg 1$  ( $i = 1, 2$ ). Thus, in the present case, both detuning parameters correctly predict the same thermodynamic limit, in this case, the vacuum state.

### 5. Final Remarks

There are a few open systems in quantum optics allowing an exact analytic solution. Our work addresses a fundamental model here, namely the generalized JCM in an optical cavity, with a complete description of the quantum state. The spontaneous decay of a spin level was treated by considering the interaction of the two-level spin system with the modes of the universe in the vacuum state. Invoking the rotation

wave approximation, the interaction picture Hamiltonian of the model can be written as the sum of two terms, one for each mode. However, these two terms fail to commute. Therefore, the non-vanishing of this commutator requires special care. Moreover, since in the present model system,  $\mathcal{H}_0$  does not commute with  $\mathcal{H}_1$ , except in the degenerate state of the field at zero detuning, the sum of those terms taken at different times also fail to commute. The different cases of interest which emerge from these non-vanishing commutation relations are associated with the relations between the detuning parameters, according to whether the whole system is in a resonant or off-resonant state, and if the cavity field is in a degenerate or nondegenerate mode. These cases were analytically implemented and numerically discussed for various values of the initial mean photon number and spin-photon coupling constants. Thus, the spin model-radiation field combined system was described through a formalism based on the expansion of the time-evolution operator matrix elements for both modes, assuming that the field states can be represented initially by the same photon distribution. Regarding an excited initial state, the dynamics of the present model was investigated via second- and third-order perturbation expansion of the time evolution operator matrix elements for the excited and ground states respectively. This required evaluation of the one-, two-, and three-times integrals involved in the chronologically ordered time perturbative Dyson expansion of the evolution operator.

The specific case of exact simultaneous resonance of both modes was treated in terms of a linearization of the expansion of the time evolution operator. This allowed us to generate explicit analytical expressions for the density operator matrix elements and the associated amplitudes. Thus, it was found that in the limit of zero detuning for both modes, the photon number distribution shows a series of peaks which collapse to a single one after an appropriate average procedure, leading then to a Poisson shaped structure peaked, as expected, at  $\langle n_1 \rangle$ . It was also found that a superposition of noncommensurate Rabi frequencies arising due to this distribution in the number of photons leads to the phenomenon of collapse and revival of Rabi oscillations. This phenomenon, which is due to the granular nature of the field, is absent if the field is considered classically.

The time evolution of the average photon number, as well as the normally ordered variances for both modes may show revivals and decays similar to those of the spin inversion under certain circumstances. These novel collapses and revivals arise from the existence of highly correlated photon states, which are produced via nonlinear optical processes. These nonclassical effects have their origin in quantum coherences established during the interaction of the spin system with the cavity field. For example, the interbeam second-order coherence is qualitatively somewhat similar to the time evolution of the population inversion computed recently by Fuli<sup>45</sup> in the study of the dynamics of the driven JCM, where a two-level atom coupled to a single mode of a cavity field driven by an external coherent field is investigated. This implies that we can examine the field statistics and the associated nonclassical effects through the interaction of the spin system with two modes of fields.



The superposition states from two-mode coherent states can exhibit other prominent nonclassical effects, such as antibunching, sub-Poissonian statistics, and violation of the Cauchy-Schwartz inequality. These nonclassical properties can be interpreted as due to the quantum interference of the coherent states in phase space, as claimed by Schleich *et al.*<sup>59</sup> In the present work, attention was concentrated in a class of two-mode nonclassical states via superpositions of two-mode coherent states. As usual, to generate these nonclassical effects in the standard JCM, one has to cool the cavity to zero temperature and prepare a coherent field in the cavity. We show that in the present generalized JCM, the nonclassical effects can be directly generated from a thermal photon state of the cavity field. The collapse and revivals of the inversion, as well as the normally ordered variances for the first and the second mode were found to be generally unaffected by the mean number of thermal photons initially present in the cavity. However, the detunings between the cavity modes and the spin system do have an important influence on the nonclassical effects. In fact, the nonclassical effect associated to the normally ordered variances can be generated by increasing the strength of the coupling spin system-cavity field, even if the mean thermal photon number is large. This was verified in the case of nonzero detuning of at least one mode. In exactly resonant states of the spin system with both modes of the cavity field, on the other hand, the sub-Poissonian statistics seem to be dominated by the photon distribution of the initial coherent state of the field. We also found a strong tendency for the two modes to be anticorrelated, which is expected, given the form of the interaction. Another investigated feature of the present generalized JCM is the possibility of exploring the influence of temperature on the photon distribution. Thus, it was found that the limit of high temperatures characterizing the manifold of excited states becomes chaotic with rapid and sharp oscillations, whereas the ground state is correctly described in the thermodynamic limit by the vacuum state.

The present generalized model admits many of the features of the usual JCM and as such, it deserves further investigation. For example, the incorporation of two-photon processes, as well as the squeezing of the field, have to be further investigated. The importance of the latter has increased recently due to its relation to quantum entanglement, a basic ingredient of quantum information. Work along these lines is planned to be reported elsewhere.

## Acknowledgments

This work has been made possible by research grants in aid from the University of Buenos Aires (Project No. X-024/05) and the Consejo Nacional de Investigaciones Científicas y Técnicas (PIP No. 05098/06). The author is grateful to the Department of Physics, Facultad de Ciencias Exactas y Naturales, Universidad de Buenos Aires, for facilities provided during the course of this work.

## References

1. S. Stenholm, *Phys. Rep. C* **6**, 1 (1973).
2. H. I. Yoo and J. H. Eberly, *Phys. Rep.* **118**, 239 (1985), and references therein.
3. E. T. Jaynes and F. W. Cummings, *Proc. IEEE* **51**, 89 (1963).
4. S. Singh, *Phys. Rev. A* **25**, 3206 (1982).
5. J. H. Eberly, N. B. Narozhny and J. J. Sánchez-Mondragón, *Phys. Rev. Lett.* **44**, 1323 (1980).
6. N. B. Narozhny, J. J. Sánchez-Mondragón and J. H. Eberly, *Phys. Rev. A* **23**, 236 (1981).
7. H. I. Yoo, J. J. Sánchez-Mondragón and J. H. Eberly, *J. Phys. A* **14**, 1384 (1981).
8. S. Stenholm, *Opt. Commun* **36**, 71 (1981).
9. S. C. Gou, *Phys. Rev. A* **40**, 5116 (1989).
10. B. Buck and C. V. Sukumar, *Phys. Lett. A* **81**, 132 (1981).
11. N. N. Bogolubov Jr., F. L. Kien and A. S. Shumovsky, *Phys. Lett. A* **107**, 456 (1985).
12. R. R. Puri and G. S. Agarwal, *Phys. Rev. A* **35**, 3433 (1987).
13. R. R. Puri and G. S. Agarwal, *Phys. Rev. A* **37**, 3879 (1988).
14. A. Joshi and R. R. Puri, *Phys. Rev. A* **42**, 4336 (1990).
15. M. Brune, E. Hagley, J. Dreyer, X. Maître, A. Maali, C. Wunderlich, J. M. Raimond and S. Haroche, *Phys. Rev. Lett.* **77**, 4487 (1996), and references therein.
16. M. Hemrich, A. Kuhn and G. Rempe, *Phys. Rev. Lett.* **94**, 053604 (2005).
17. C. W. Gardiner and P. Zoller, *Quantum Noise*, 2nd edn. (Springer, Berlin, 2000).
18. F. Bloch and A. J. Siegert, *Phys. Rev.* **57**, 522 (1940).
19. P. Goldberg and L. C. Harrison, *Phys. Rev. A* **43**, 376 (1991).
20. C. K. Law, T. W. Chen and P. T. Leung, *Phys. Rev. A* **61**, 023808 (2000).
21. C. K. Law and J. H. Eberly, *Phys. Rev. Lett.* **76**, 1055 (1996).
22. M. Lewenstein, Y. Zhu and T. W. Mossberg, *Phys. Rev. Lett.* **64**, 3131 (1990).
23. Y. Zhu, Q. Wu, S. E. Morin and T. W. Mossberg, *Phys. Rev. Lett.* **65**, 1200 (1990).
24. D. A. Holm, M. Sargent III and S. J. Stenholm, *J. Opt. Soc. Am. B* **2**, 1456 (1985).
25. M. Lewenstein and T. W. Mossberg, *Phys. Rev. A* **38**, 1075 (1988).
26. M. Sugahara and S. Kruchinin, *Mod. Phys. Lett. B* **15**, 473 (2001).
27. Y. Makhlin, G. Schön and A. Shnirman, *Rev. Mod. Phys.* **73**, 357 (2001).
28. S. A. Wolf, D. D. Awschalom, R. A. Buhrman, J. M. Daughton, S. von Molnár, M. L. Roukes, A. Y. Chtchelkanova and D. M. Treger, *Science* **294**, 1488 (2001).
29. P. Ball, *Nature* **404**, 918 (2000).
30. D. Bouwmeester, A. Ekert and Z. Zeilinger (eds.), *The Physics of Quantum Information: Quantum Cryptography, Quantum Teleportation, Quantum Computation* (Springer-Verlag, Berlin, 2000).
31. A. N. Chaba, M. J. Collet and D. F. Wall, *Phys. Rev. A* **46**, 1499 (1992).
32. J. I. Cirac, R. Blatt, A. S. Parkings and P. Zoller, *Phys. Rev. A* **49**, 1202 (1994).
33. N. V. Bordyug and V. P. Krainov, *Laser Phys. Lett.* **4**, 674 (2007).
34. C. C. Gerry and J. H. Eberly, *Phys. Rev. A* **42**, 6805 (1990).
35. C. C. Gerry and R. F. Welch, *J. Opt. Soc. Am. B* **9**, 290 (1992).
36. N. Bloembergen and Y. R. Shen, *Phys. Rev. A* **37**, 133 (1964).
37. B. R. Mollow, *Phys. Rev. A* **5**, 2217 (1972).
38. C. K. Law and J. H. Eberly, *Phys. Rev. A* **43**, 6337 (1991), and references therein.
39. D. A. Cardimona, V. Kovanis, M. P. Sharma and M. P. Gavrielides, *Phys. Rev. A* **43**, 3710 (1991).
40. H. Grinberg, *Phys. Lett. A* **344**, 170 (2005).
41. H. Grinberg, *Phys. Lett. A* **350**, 428 (2006).
42. H. Grinberg, *Int. J. Quantum Chem.* **106**, 1769 (2006).

43. E. Lieb, T. Schultz and D. Mattis, *Ann. Phys.* **16**, 407 (1961).
44. H. Grinberg, *Int. J. Quantum Chem.* **108**, 210 (2008).
45. F.-L. Li and S.-Y. Gao, *Phys. Rev. A* **62**, 043809 (2000).
46. C.-L. Chai, *Phys. Rev. A* **46**, 7187 (1992).
47. Y.-G. Li, P. J. Edwards, X. Huang and Y. Wang, *J. Opt. B* **2**, 292 (2000).
48. Z. Ficek and R. Tanas, *Phys. Rep.* **372**, 369 (2002).
49. P. G. O. Anicich and H. Grinberg, *Int. J. Quantum Chem.* **90**, 1562 (2002).
50. H. Grinberg, *Phys. Lett. A* **311**, 133 (2003).
51. W. H. Louisell, *Quantum Statistical Properties of Radiation* (Wiley, New York, 1990).
52. K. J. Resch, J. S. Lundeen and A. M. Steinberg, *Phys. Rev. A* **63**, 020102 (2001).
53. Y. J. Lu and Z. Y. Ou, *Phys. Rev. Lett.* **88**, 023601 (2002).
54. H. F. Hofmann, *Phys. Rev. A* **70**, 023812 (2004).
55. A. B. U'Ren, C. Silberborn, J. L. Ball, K. Banaszek and I. A. Walmsley, *Phys. Rev. A* **72**, 021802 (2005).
56. J. Xiong, N. Zhou and G. Zeng, *J. Phys. B* **38**, 4301 (2005).
57. M. D. Reid and D. F. Walls, *Phys. Rev. A* **34**, 1260 (1986).
58. R. N. Deb, M. Sebawe Abdalla, S. S. Hassan and N. Yayak, *Phys. Rev. A* **73**, 053817 (2006), and references therein.
59. W. Schleich, M. Pernigo and F. L. Kien, *Phys. Rev. A* **44**, 2172 (1991).